ATTACKING THE HIV EPIDEMIC FROM ALL SIDES: OPTIMIZATION OF PCR STRATEGIES TO MEASURE CLONAL EXPANSION AND QUANTITATIVE EVALUATION OF DOLUTEGRAVIR

by
Sarah Laskey

A dissertation submitted to Johns Hopkins University in conformity with the requirements for the degree of Doctor of Philosophy

Baltimore, Maryland
June 2016

Abstract

Although great progress has been achieved in the fight against HIV and AIDS, an epidemic continues to rage worldwide. Alongside public health and clinical efforts, scientific research plays a major role in this fight; ongoing studies focus on improving treatment options, designing a vaccine, and developing a cure. The first study described in this dissertation is a critique of research and analysis methods commonly used to characterize the latent HIV reservoir, which is considered a barrier to the cure of HIV infection. This project highlights the importance of understanding molecular biology tools and considering their inherent limitations when interpreting results. The second study presented here comprises a quantitative evaluation of the efficacy of dolutegravir, an antiretroviral drug that has emerged recently as one of our best weapons for controlling HIV infection. Results show that the high efficacy of dolutegravir in combination with other antiretroviral drugs, as well as the high genetic barrier to viral evolution of dolutegravir resistance, are consistent with the tremendous clinical success of this drug. The grand conclusion of this dissertation is that much work remains to be done. We continue to discover safer, more effective tools for the treatment of HIV infection, which may be seen as a silver lining given how far we appear to be from achieving a cure.

Thesis Committee:

Dr. Robert Siliciano (Thesis Advisor, Reader)

Dr. Stuart Ray (Committee Chair, Reader)

Dr. Joel Blankson

Dr. Winston Timp

Acknowledgments

I would first like to thank my advisor, Robert Siliciano. For so many reasons, the work described here would not have been possible without him. The environment of the Siliciano Lab—for which I must also thank Janet Siliciano—is one where my research was limited only by the scope of my imagination and the hours in the day. For their unwavering support and guidance as I insisted on dreaming up my own projects and then carried them out with abandon, I am forever grateful to Bob and Janet.

More thanks to my thesis committee members, Stuart Ray, Joel Blankson, and Winston Timp for making time in their impossibly busy lives to listen to my ideas, provide valuable feedback, and then bear with me when my research forged a completely unrelated path of its own. It was an honor and so much fun to share my work with this brilliant group. A special thanks to Stuart Ray for all of the above and for confirming my sanity in times of crisis.

I also want to thank the entire BME department, especially Hong Lan, whose careful, personal attention to hundreds of students at a time has never ceased to amaze me, and who was always ready with answers before I even figured out what question to ask.

Thanks to every person who donated blood to make the studies in this dissertation (and the ones that never made it as far as publication) possible.

I am sure my undergraduate mentors Paul Boutz and Mohini Jangi will never read this, but they are more than deserving of my gratitude. They put up with my embarrassingly immature twenty-year-old self and taught me all of the tools I needed to hit the ground running in my graduate lab. They were so much better to me than I deserved, and I still strive to be someone they would respect.

Thanks to my lab mates. Thanks to the older students, especially Maame Sampah and Korin Bullen, who showed me the ropes and put up with incessant questions when I was new. Thanks to every phlebotomist I ever inconvenienced for a blood draw. Thanks to everyone who attended Friday meetings, especially Katie Bruner and Andrew Timmons, for their enthusiastic and enlightening conversation.

I would also like to thank the Biomedical Odyssey blog and everyone involved there, especially Bree Yanagisawa. I have never considered myself much of a writer, but I am proud of what this group has accomplished and grateful to have been a part of it. Also apparently it looks great on my resume.

There are not enough words in the dictionary or breaths in a lifetime (or keys on a laptop?) to express how grateful I am to my family for their love, their support, and their friendship. To my grandmother for her vibes, to my father for his guidance and constancy, to my mother for her never-ending advice, perspective, and help on my homework. To my siblings, my first and best friends. To Allison for her wisdom and her sympathy, to Rob for his wit and his thoughtfulness, to Hannah for her strength and her sensibility. Without every one of you, the person I am (and her meager achievements) would not be.

Last and perhaps most, thanks to Chris Pohlmeyer, who would probably prefer that this acknowledgment be kept to a minimum. I will say only that you are my partner in everything, including but not limited to my research.

"It even was suggested that the production of a suitable number of bricks was equivalent to building an edifice and therefore should entitle the industrious brickmaker to assume the title of builder and, with the title, the authority...And, saddest of all, sometimes no effort was made even to maintain the distinction between a pile of bricks and a true edifice."

Bernard K Forscher
Chaos in the Brickyard
Science
1963

Preamble

The chapters of this dissertation comprise manuscripts prepared for publication. They are self-contained, and each includes introduction and discussion sections to contextualize and interpret the data presented. For the broader, dissertation-level introduction and discussion sections required by my department, I have presented a bird's-eye view of HIV research from my own perspective, informed by the five years I spent in the field. These sections are written in a style somewhere between opinion article and memoir.

The opinions presented here represent only my own; in fact, I expect them to annoy some of my readers. Nevertheless, this may be my only opportunity to publish what I believe are the most important insights from my graduate career without the burden of co-authors to appease. The fact that my perspective seems so frequently to diverge from that of my colleagues may suggest that I am a visionary; more likely, it means I am wrong. From my readers, I beg an open mind or, failing that, their forgiveness.

Table of Contents

List of Tables

List of Figures

Introduction

The fantastically rapid discovery, development, and approval of effective antiretroviral therapy (ART) for the treatment of HIV may be one of the greatest accomplishments ever achieved by medical science. Likewise, in the words of the World Health Organization, “the global health response to HIV represents one of the greatest public health feats of recent times.” The rate of new HIV infections and the frequency of HIV-related deaths worldwide have been decreasing for over a decade, while the number of infected people with access to treatment continues to rise [1]. However, the national and international medical communities foster no illusions that the HIV epidemic is under control.

In 2014, over one million people worldwide died from causes related to HIV infection. The same year, two million more people were infected with the virus, which is the etiological agent responsible for the immunodeficiency disease known as AIDS. In 2014, zero people living with HIV were cured of their infection. The math is simple, but the implications are profound; the number of people worldwide living with HIV infection increased by almost one million in 2014 [1].

At the beginning of the HIV/AIDS epidemic, the most urgent and important task at hand was the management of people being infected with HIV and dying from AIDS. In recent years, thanks in large part to enormous strides in HIV treatment, this focus has broadened to encompass a new, expanding population in need of resources and attention, the population of people *living with* HIV.

I know of four ways that the scientific and medical establishments can contribute to the global response against HIV:

1. A continued public health effort to bring HIV testing, treatment, and prevention to affected communities.

2. The development of new antiretroviral drugs with novel mechanisms of action and/or improved toxicity profiles, decay rates, or price points.
3. The development of a vaccine (or functional vaccine) to prevent new infections in high-risk populations.
4. The development of a cure (or functional cure) to reduce the number of infected persons and at least partially alleviate the need for antiretroviral drugs.

The first of these four can be achieved with strategies and technologies that already exist, although it may be expedited by the development of newer, better tools. The latter three goals require novel scientific innovation. The two chapters of this dissertation describe two different projects intended to contribute to the second and fourth goals in the above list. While the work presented here will almost certainly have zero impact on the lives of HIV-infected people or their communities, it nevertheless represents a small contribution to the volumes of scientific publications produced (ostensibly) with that intent.

Chapter I: Evaluating Clonal Expansion of HIV-infected Cells

Abstract

In HIV-infected individuals receiving suppressive antiretroviral therapy, the virus persists indefinitely in a reservoir of latently infected cells. The proliferation of these cells may contribute to the stability of the reservoir and thus to the lifelong persistence of HIV-1 in infected individuals. Because the HIV-1 replication process is highly error-prone, the detection of identical viral genomes in distinct host cells provides evidence for the clonal expansion of infected cells. We evaluated alignments of unique, near-full-length HIV-1 sequences to determine the relationship between clonality in a short region and clonality in the full genome. Although it is common to amplify and sequence short, subgenomic regions of the viral genome for phylogenetic analysis, we show that sequence identity of these amplicons does not guarantee clonality across the full viral genome. We show that although longer amplicons capture more diversity, no subgenomic region can recapitulate the diversity of full viral genomes. Consequently, some identical subgenomic amplicons should be expected even from the analysis of completely unique viral genomes, and the presence of identical amplicons alone is not proof of clonally expanded HIV-1. We present a method for evaluating evidence of clonal expansion in the context of these findings.

Author Summary

Although antiretroviral therapy effectively blocks HIV-1 replication, the virus persists indefinitely in a reservoir of latently infected cells. This reservoir is a major barrier to HIV-1 cure. Recent studies have identified the proliferation of latently infected cells as a mechanism that may contribute to the lifelong persistence of HIV-1. In contrast with cellular proliferation, viral replication is highly error-prone; therefore, the detection of identical viral genomes in distinct host cells provides evidence that those

cells are the progeny of an infected cell that underwent clonal expansion. For this reason, the accurate and reliable identification of identical HIV-1 genomes derived from distinct cells is critical for understanding HIV-1 persistence and advancing cure research. Studies of HIV-1 clonal expansion often present clonality of short, subgenomic sequences as evidence for the clonality of full viral genomes. In this study, we quantified the relationship between sequence identity in short regions and sequence identity of near-full-length genomes to demonstrate that no subgenomic region completely captures the diversity of the full viral genome. Consequently, identical subgenomic sequences are not proof of identical full-length HIV-1 genomes. In the context of these findings, we developed a method to evaluate identical subgenomic sequences as possible evidence for clonal expansion.

Introduction

The HIV-1 virion carries two copies of a 9.7 kb RNA viral genome, which is reverse transcribed to DNA and integrated into the genome of a host cell during infection. Although combination antiretroviral therapy (ART) can suppress HIV-1 plasma viremia indefinitely to a level below the clinical limit of detection, the virus persists for decades in a latent reservoir composed of resting memory $CD4^+$ T cells carrying integrated viral genomes, known as proviruses [2-5]. The development, composition, and plasticity of this latent reservoir, which presents a major barrier to the cure of HIV-1 infection, are all active areas of investigation [6,7].

An emerging body of research identifies the proliferation of latently infected $CD4^+$ T cells as a possible mechanism for the persistence—and perhaps expansion—of the latent reservoir. Because viral replication is a low-fidelity process, expansion of the reservoir through cellular proliferation can be distinguished from expansion through *de novo* infection events by the presence of identical HIV-1 genomes with identical sites of integration into the host cell genome in distinct cells [8-10].

In part due to the substantial diversity of HIV-1 even within a single infected individual, generating full-length sequences of individual proviruses can be prohibitively expensive and labor intensive. Instead, it is common to sequence short PCR amplicons covering less than 3000 base pairs [8,9,11-19]. While these smaller, subgenomic amplicons contain sufficient sequence information to inform phylogenetic analysis, they do not capture the total diversity–in this case, defined as the proportion of non-clonal sequences—present in full-length viral genomes from the same sample. On the contrary, the sequence diversity in a subgenomic region is best understood as a minimum estimate of the total sequence diversity in the sample analyzed. Without comparing full-length HIV-1 genomes, it is impossible to determine whether two proviruses with identical sequence over a subgenomic amplicon are also identical over the remainder of the viral genome.

This inherent overestimation of viral clonality when comparing short, subgenomic sequences is of critical importance in the investigation of clonal expansion of latently infected cells as a mechanism of HIV-1 persistence. A number of studies have identified identical viral sequences in independent samples from a single subject [8,9,14,18-21]. These identical sequences may reflect the expansion of latently infected $CD4^+$ T cells *in vivo*. However, when the identical sequences analyzed cover only a short fragment of the viral genome, they may also represent distinct infection events with viral genomes that happen to differ only in areas of the genome that were not analyzed. This distinction underscores the importance of understanding the relationship between the sequence diversity in subgenomic PCR amplicons and that of full viral genomes.

The goal of this study was to identify which short PCR amplicons—if any—capture the total diversity of full-length genomes in a sample. We analyzed near-full-length HIV-1 sequences available from previous studies; importantly, we specifically characterized intra-subject diversity. We considered how length, genomic position, and sample type contribute to the likelihood that a given subgenomic amplicon will include enough information to differentiate unique, full-length HIV-1 sequences. Given these findings,

we characterized and evaluated eight PCR primer sets used in previously published studies of HIV-1 diversity for their ability to differentiate full-length viral sequences. We showed that subgenomic sequences are contextualized by the primer set used to generate them, and we present here a strategy for the evaluation of sequence data in the context of specific primer sets.

Results

Data sets and processing. We analyzed data sets containing between 5 and 121 (mean=20.7, median=9) unique, near-full-length HIV -1 sequences from a total of 31 subjects. None of the sequences analyzed cover the 5' LTR, and all sequences are fully characterized at a minimum from positions 2000 through 8000 of the HXB2 reference genome. These sequences represent five different sample types: 1) proviral DNA from the resting $CD4^+$ T cells of subjects who initiated suppressive ART during acute HIV-1 infection, designated "Acute treated – DNA"; 2) proviral DNA from the resting $CD4^+$ T cells of subjects who initiated suppressive ART during unspecified stages of chronic HIV-1 infection, designated "Chronic treated – DNA"; 3) proviral DNA isolated from quantitative viral outgrowth assay (VOA) [22] wells negative for p24 antigen, representing resting $CD4^+$ T cells that were not induced to produce replication-competent virus after stimulation with phytohemagglutinin, designated "VOA – DNA"; 4) genomic viral RNA isolated from the plasma of viremic subjects over a series of longitudinal time points, designated "Longitudinal – RNA"; and 5) genomic viral RNA isolated from the plasma of subjects during acute HIV-1 infection, designated "Acute – RNA." The data sets were aligned to the HXB2 reference HIV-1 genome and processed to remove repeat sequences. Sequences were characterized as repeats if they were identical or differed only at ambiguously sequenced positions for all nucleotides sequenced. Thus, every full-genome sequence is unique in the alignments analyzed below. Details about sequence data sets and their sources are shown in Table 1 and Table 3. We have shown that our results are not sensitive to the specific alignments; that is, the results are equivalent for different but equally probable

Table 1. Sources and characteristics of sequence alignments analyzed to generate clonal prediction scores.

Sample	Source	Reference	PMID	Number of subjects	Sequences per subject (range)
Acute treated – DNA	DNA from resting $CD4^+$ T cells of subjects treated during acute infection	Bruner *et al*., manuscript under revision [29]	-	6	7-14
Chronic treated – DNA	DNA from resting $CD4^+$ T cells of subjects treated during chronic infection	Bruner *et al*., manuscript under revision [29]	-	5	8-13
VOA – DNA	DNA from p24 antigen-negative quantitative viral outgrowth assay [22] culture wells	Ho *et al*., 2013, Cell. [23]	24243014	5	6-12
Longitudinal – RNA	Plasma RNA from 2-10 longitudinal samples per subject	Herbeck *et al*., 2011, J. Virol. [16]	21593162	6	28-121
Acute – RNA	Plasma RNA collected during acute infection	Salazar-Gonzalez *et al*., 2009, J. Exp. Med. [15]	19487424	9	5-14

alignments of the same sequences (Figure 5). For this study, only alignments including at least five unique, full-length HIV-1 genome sequences from the same individual were considered.

Because our goal was to characterize intra-subject diversity, we analyzed the alignments from each subject individually. Figure 1a shows a schematic of our analytic procedure. We considered a series of hypothetical primer pairs defining subgenomic PCR amplicons. Each of these primer sets was evaluated against each subject sequence alignment. We assumed that a sequence could be amplified by a primer set if the sequence aligned to the HXB2 reference genome without any gaps in either primer site.

For each sequence alignment, we considered the amplicons that would be produced by a PCR with a given hypothetical primer set, discarding the sequences that would not be amplified by that primer set due to insertions or deletions overlapping the primer binding sites. We chose to consider only PCR-amplifiable sequences to maximize the practical value of our metric for the analysis of sequence data sets generated using PCR-based protocols. We defined the *clonal prediction score* (CPS) of the primer set as the number of unique amplicons produced, divided by the total number of amplicons produced, and multiplied by 100 (Figure 1a). In words, the CPS of a primer set with respect to an alignment is defined as the percentage of sequences in the alignment that would be correctly identified as unique using only the sequence region amplified by those primers. Each full genome in these alignments is unique, and primer sets that produce a unique amplicon for every amplifiable sequence in the alignment have a CPS of 100.

These parameters define a maximal CPS of 100 and a minimum possible CPS of $100/N$, where N is the number of amplified sequences. When a primer set will not amplify any of the sequences in an alignment, the CPS is undefined for that primer set with respect to that alignment. Undefined CPS values are excluded from the figures described below. Importantly, the precision of the CPS is limited

Figure 1. Clonal prediction scores of 1 kb amplicons spanning the HIV-1 genome. (**a**) Schematic of algorithm to calculate clonal prediction score (CPS), which quantifies the proportion of unique sequences in an alignment that are correctly identified as unique using the amplicons produced by a specific primer set. (**b**) CPS of 1 kb-wide amplicons spanning the HIV-1 genome for six Acute treated – DNA subjects. (**c**) CPS of 1 kb-wide amplicons spanning the HIV-1 genome, averaged over all subjects in five different sample categories (Table 1). (**d**) Overlay of the five plots in part **c**. Schematics of the HIV-1 genome are aligned to the charts in parts **b** through **d** to highlight viral gene locations. The amplicons in parts **b** through **d** are defined with reference to the HXB2 genome.

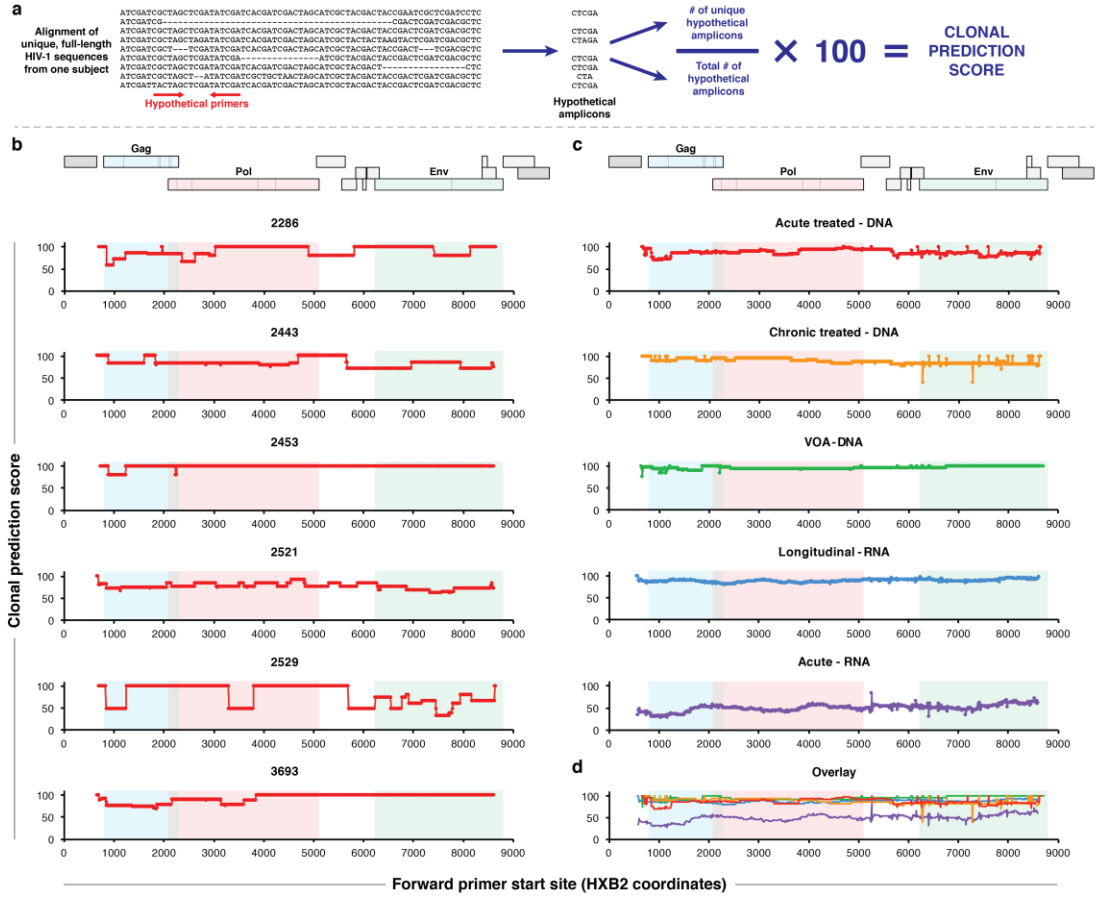

by the number of sequences amplified by a primer set. For example, a primer set that correctly distinguishes 5 of 5 amplicons would have the same perfect CPS = 100 as a primer set that correctly distinguishes 100 of 100 amplicons. If a new unique sequence were added to the alignment and incorrectly identified as clonal, the CPS values in these two cases would change to 83 and 99, respectively. For this reason, the empirically perfect CPS = 100 may be more precisely described as CPS > 100*N/(N+1). This example emphasizes why alignments containing more sequences lead to greater precision in CPS values. For clarity, we have plotted maximal CPS values at CPS = 100 in the figures described below.

Substantial variation in CPS among subjects. To investigate how CPS varies across the HIV-1 genome and across infected individuals, we calculated CPS values for hypothetical 1 kb amplicons spanning the HIV-1 genome at 10 bp intervals. These amplicons were defined by hypothetical 10 bp forward and reverse primers, and we have shown that the results of the following analysis are not sensitive to the choice of primer length (Figure 6). While the amplicons defined by these hypothetical primers have a length of 1 kb in the HXB2 reference genome, they may have different lengths in sequences containing insertions or deletions between the primer sites. Along with sequence differences, length polymorphisms can be used to differentiate unique sequences.

The results of this analysis for six Acute treated – DNA samples (Table 1) are shown in Figure 1b. There was substantial variation among subjects, suggesting that a primer set optimized to differentiate sequences in one sample may not be optimal in another sample from a different subject. For subject 2453, almost every 1 kb amplicon contained sufficient variation to differentiate all amplified sequences, but the other five subjects had CPS values below 100 for amplicons spanning large portions of the genome. For subject 2521, less than one percent of all possible 1 kb amplicons had a perfect CPS of 100. That is, almost every 1 kb amplicon would incorrectly classify unique genomic sequences from subject

2521 as identical. There is no relationship between these patterns and the number of sequences analyzed for each subject (Figure 7 and Table 3).

Plots of CPS across the genome for individual Chronic treated – DNA, VOA – DNA, Longitudinal – RNA, and Acute – RNA samples (Table 1) are shown in Figure 7. The perfect CPS of 100 is much more common for proviral DNA than for plasma RNA; in Chronic treated – DNA and VOA – DNA samples, more than half of subjects had perfect CPS values for every 1 kb amplicon across the viral genome. These perfect CPS values are often found at locations in the genome where one or more sequences in the alignment contain deletions and cannot be amplified. In these cases, the total number of sequences detected by a primer set (the denominator in the CPS equation) is lower, and there are fewer amplicons to be differentiated. Although alignments containing only a few sequences do not lead to bias or inaccuracy in the CPS, the precision of the CPS calculation is correlated with the number of sequences in the alignment being analyzed. In the compilation of our data set, we chose to include only subjects for whom at least five unique, near-full-length sequences had been characterized, but the precision of these results would be improved by the collection and inclusion of more sequences per subject.

The dramatic variation in CPS among different subjects is seen in all sample types assayed except Longitudinal – RNA (Figure 7). For Longitudinal – RNA samples, CPS is consistent between subjects and across the viral genome. This result reflects the high diversity of the HIV-1 quasispecies during chronic infection.

Lack of genomic hotspots for CPS across sample types. To determine whether optimized primer sets for the identification of clonal HIV-1 sequences should be located in specific regions of the viral genome, we plotted the CPS for hypothetical 1 kb amplicons spanning the HIV-1 genome, averaged over all of the subjects within each sample group (Figure 1c). The top plot in Figure 1c shows the average of the six plots in Figure 1b, and the other plots in Figure 1c show averages of the plots in Figure 7. Figure 1d is an

overlay of the five plots in Figure 1c. The purpose of these averaged scores was to determine whether any region of the viral genome yields consistently higher or lower CPS than other regions across different subjects or sample types.

CPS values averaged over several subjects are relatively consistent across the viral genome for all five sample types evaluated. In the Acute treated – DNA and Chronic treated – DNA samples, CPS values appear slightly higher for the 5' half of the genome than for the 3' half. In contrast, the CPS for VOA – DNA samples is highest at the 3' end of the genome. Importantly, these general trends are not representative of individual subjects, *e.g.*, Acute treated – DNA subject 3693 has a perfect 100 CPS only for amplicons toward the 3' end of the viral genome (Figure 1b).

The Acute – RNA samples stand out as having lower CPS values across the viral genome than the other sample types (Figure 1d), indicating that the sequences in these alignments differ at relatively few places in the genome. This finding is consistent with the biological characteristics of the Acute – RNA sample type; these sequences contain low genetic diversity because they represent plasma collected during acute HIV-1 infection, before the viral quasispecies has expanded and developed the sequence diversity characteristic of chronic infection. In most individuals, HIV-1 infection is initiated by a single transmitted founder virus that expands into a diverse quasispecies over the course of untreated infection [23,24].

Importantly, these results show that there is no optimal region of the genome best suited for differentiating unique sequences in a subject- or sample type-independent manner.

Effect of amplicon length on CPS. To determine the effect of amplicon length on CPS, we calculated the CPS for hypothetical amplicons of different lengths spanning the HXB2 genome. We summarized the analysis of all amplicons of a given length in three ways, by taking the average, median, and minimum

CPS over all amplicons of that length across the genome (Figure 2a). For example, all of the points plotted in the top chart from Figure 1b are averaged together to yield the subject 2286, 1000 bp data point in the Acute treated – DNA Average CPS plot in Figure 2a. Individual results for the 31 subjects are grouped by sample type.

For every subject, regardless of sample type, longer amplicons yield higher CPS. This is unsurprising, as a longer amplicon should be more likely than a short amplicon to contain sequence diversity. However, the precise relationship between amplicon length and CPS varies dramatically by sample type. In proviral DNA samples, CPS increases with amplicon length but varies among subjects. For very short amplicons between 100 bp and 500 bp, average and median CPS can range from about 40 to a perfect 100. For very large amplicons of 6 kb, the average CPS is greater than 80 and the median CPS is 100 for almost every proviral DNA sample. Again, there is no correlation between CPS and the number of amplicons in a sequence alignment (Figure 2 and Table 3).

In DNA from subjects treated during chronic infection, the relationship between amplicon length and CPS is similar for three of five subjects. CPS values are high for the three Chronic treated – DNA samples that cluster together in Figure 2; all three subjects have a perfect CPS of 100 across the viral genome for amplicons as short as 1 kb. Subject CP03 is believed to have initiated therapy early in chronic infection, which may explain the similarity of that sample to the Acute treated – DNA samples. Subject CP10 illustrates an important limitation of any sequence-based analysis. Two of the sequences in the CP10 alignment differ by a single nucleotide. These sequences likely represent identical genomes that differ because of an error generated during PCR, but they were considered to be unique for this analysis. Because the error rate of PCR using high-fidelity polymerases is of a much lower magnitude than HIV-1 sequence diversity, our results overwhelmingly reflect true viral diversity (rather than technical diversity) except in this exceptional case of PCR error in identical genomes.

Figure 2. Relationship between amplicon length and CPS. Summary statistics describing all amplicons of a given length, spanning the HXB2 reference genome at 10 bp intervals. Amplicons with undefined CPS were not included in these summary statistic calculations. (**a**) Average, median, and minimum of the CPS values for every amplicon of a specified length spanning the viral genome. Summary statistics are shown for each subject and grouped by sample type. (**b**) Proportion of all of the amplicons of a specified length that have CPS values above 80.

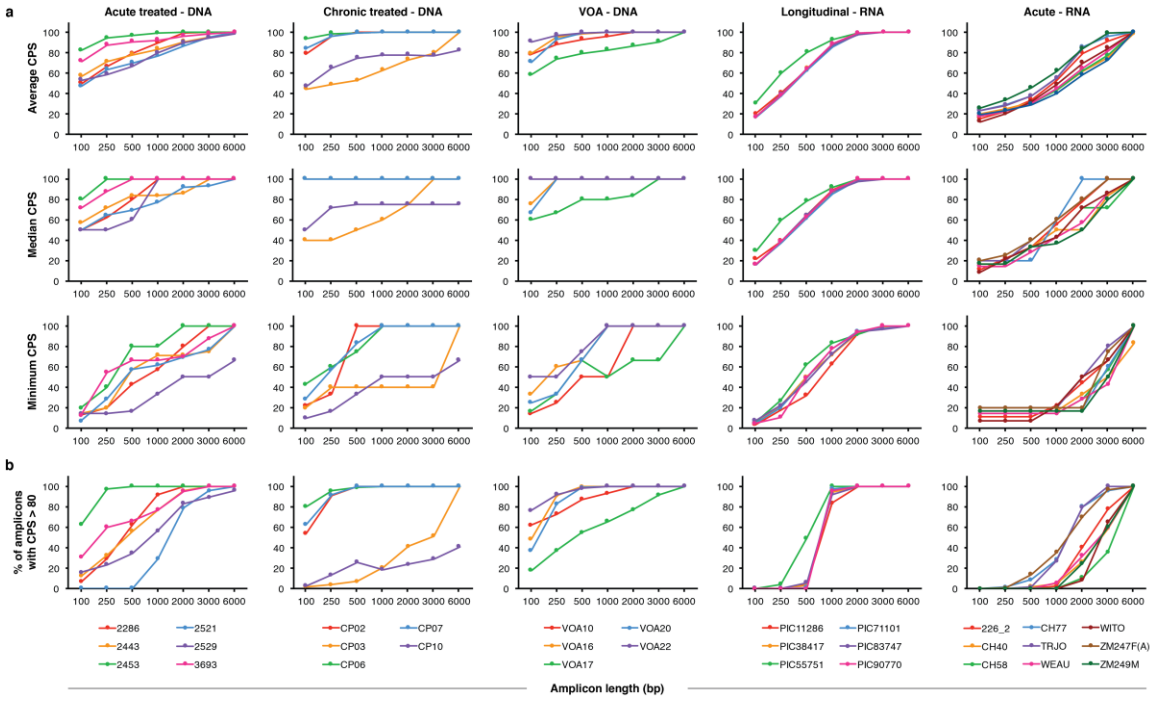

In plasma RNA samples, the relationship between amplicon length and CPS is direct and consistent across subjects. Unlike with the proviral DNA samples, the average and median CPS for plasma RNA can be lower than 20 for 100 bp amplicons. These low CPS values indicate alignments with many detectable sequences but insufficient sequence diversity to distinguish them using small amplicons.

The relationship between amplicon length and CPS is direct and linear for Longitudinal – RNA samples. There is much less inter-subject variation in this relationship for Longitudinal – RNA than for any of the other sample types. Importantly, even the minimum CPS increases predictably with amplicon length for these samples. For all Longitudinal – RNA samples, the average CPS is greater than 95 for 2 kb amplicons, and even the minimum CPS for a 2 kb amplicon is greater than 90. This contrasts with the other sample types, where average CPS increases predictably with amplicon length but minimum CPS is variable.

Figure 2a shows that most short PCR amplicons are limited in their capacity to distinguish unique HIV-1 genomes, and that the goal of a single short amplicon with a perfect CPS of 100 in a variety of subjects and sample types is unattainable. Instead, we evaluated how many amplicons achieve high—but not necessarily perfect—CPS values. Figure 2b shows the proportion of amplicons of a given length with CPS > 80. The relationship between amplicon length and the frequency of amplicons with CPS > 80 is largely consistent with the results shown in Figure 2a but emphasizes the inter-subject differences in CPS patterns.

Variation in PCR coverage with sample type and amplicon length. Importantly, CPS is undefined for a primer set that will not amplify any of the sequences in a given alignment. The summary statistics in Figure 2 describe only the primer sets with defined CPS for each subject. In other words, the CPS values shown in Figure 2 represent only the primer sets for which at least one sequence in the alignment is detectable. We calculated PCR coverage, or the fraction of sequences in each alignment that would be

detectable by PCR, averaged over all amplicons of a given length between HXB2 coordinates 2000 and 8000 (Figure 3). We chose this region because it is fully characterized for every sequence in our data set, and so the data in Figure 3 reflect the presence of internal deletions in the sequences rather than missing sequence data. As described above, we considered amplicons defined by hypothetical primer sets spanning the region at 10 bp intervals.

The PCR coverage reflects the overall percentage of the viral genome lost to internal deletions in each sample. This value is consistent across subjects in plasma RNA samples (Figure 3), for all of which the proportion of detectable amplicons approaches 100%, especially with very large 6 kb amplicons. Plasma RNA represents viral genomes capable of producing all of the viral proteins necessary to generate a functional virion and therefore does not contain large internal deletions. In contrast, proviral DNA samples are much less likely to be detected by PCR because of the high frequency of large internal deletions in archived proviral genomes [25]. There is substantial variation in PCR coverage for proviral DNA samples among different subjects and across sample types. On average, Acute treated – DNA sample sequences are more likely to be detected by PCR than Chronic treated – DNA or VOA – DNA sample sequences.

The results shown in Figure 3 have implications for primer design independent of CPS. In proviral DNA samples, the results of PCR-based analyses may vary dramatically with the choice of primers because different sequences in the sample can be intact or deleted in different regions of the viral genome; bias may be introduced by the specific selection of only the sequences that happen to be intact in a particular region.

CPS of previously published amplicons. We calculated the CPS for eight primer sets used in published studies of HIV-1 diversity, evolution, and clonal expansion (Table 2) with respect to the sequence alignments in our data set. The results, averaged over all subjects for each sample type, are presented

Figure 3. Relationship between amplicon length and PCR coverage. Percentage of sequences in each alignment that would be detectable by PCR, averaged over all amplicons of a specified length spanning HXB2 positions 2000 through 8000 at 10 bp intervals. Results are shown for 31 subjects and grouped by sample type (Table 1).

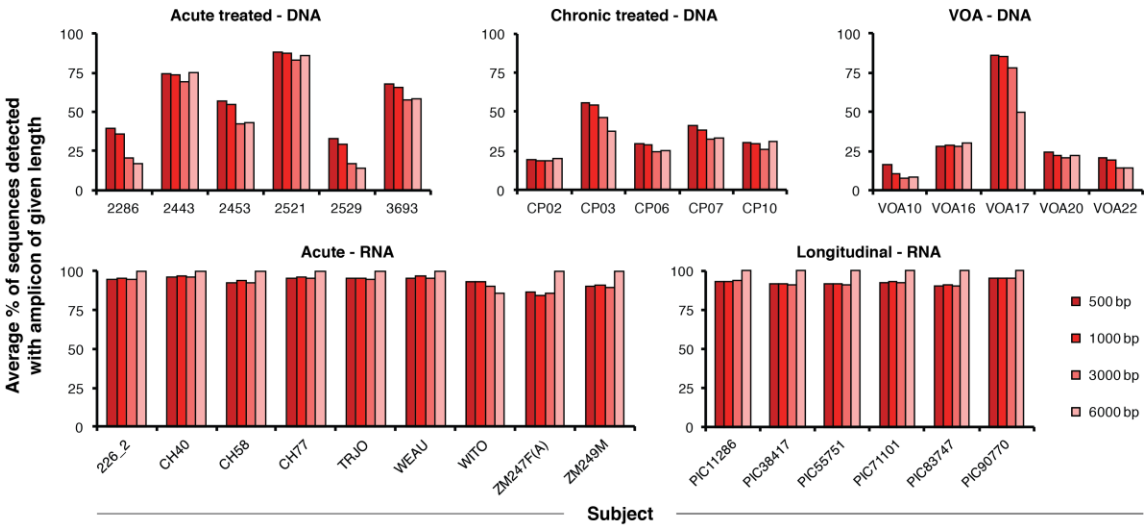

Table 2. Amplicons from published studies of HIV diversity, evolution, and clonal expansion.

Primer set	Reference	PMID	Amplicon length (bp)	Amplicon HXB2 coordinates	F primer	R primer
env 1	Evering *et al.*, 2012, PLoS Pathog. [17]	22319447	2948	5956 – 8903	TTAGGCATCTCCTATGGCAGGAAGAAG	GTCTCGAGATACTGCTCCCACCC
p6-gag-pro	Palmer *et al.*, 2005, J. Clin. Microbiol. [13]	15635002	1565	1870 – 3434	GAGTTTTGGCTGAAGCAATGAGCC	TTAGTGGTACTACTTCTGTTAGTGTT
pol 1	Bailey *et al.*, 2006, J. Virol. [14]	16775332	664	2598 – 3261	AYGGCCCAARAGTYAAAC	TTATCAGGATGGAGYTCA
env 2	Delwart *et al.*, 1993, Science [11]	8235655	667	7001 – 7667	CTGTTAAATGGCAGTCTAGC	CACTTCTCCAATTGTCCCTCA
pro	Bailey *et al.*, 2006, J. Virol. [14]	16775332	537	2056 – 2592	TGAAAGATTGTACTGAGAGACAGG	CCTGGCTTTAATTTTACTGGTACAG
env 3	Bailey *et al.*, 2006, J. Virol. [14]	16775332	471	1059 – 7529	ACAATGCTAAAACCATAATAGT	CATACATTGCTTTTCCTACT
pol 2	Wagner *et al.*, 2013, J. Virol. [18]	23175380	416	2200 – 2615	CTCCCCCTCAGAAGCAGGAGCCG-ATAGACAAGGAACTGTATCC	GGATGGCCCAAAAGTTAAAC
gag (SCA)	Palmer *et al.*, 2003, J. Clin. Microbiol. [12]	14532178	79	1298 – 1376	CATGTTTTCAGCATTATCAGAAGGA	TGCTTGATGTCCCCCCACT

in Figure 4a. Consistent with the results in Figure 2, larger amplicons typically have higher CPS values, and this relationship is most distinct in plasma samples. Importantly, in most of the samples shown, none of the published primer sets have a perfect CPS of 100. Consequently, in any analysis of sequences derived using these primers, some unique full-length genomes will be misrepresented as identical amplicons.

Using CPS to quantify false-positive clonality. The analysis of subgenomic amplicons to characterize HIV-1 genomes cannot provide definitive evidence of clonality in a sample, even when identical sequences are detected. The CPS for a primer set indicates how much false-positive clonality is found by that primer set in alignments of unique genomes. Thus the CPS for alignments of unique genomes can be understood as an estimate of the background signal expected when using a given primer set to evaluate clonality. We used the CPS of published primer sets to estimate the presence or absence of true clonality in published phylogenetic trees. This analysis is described in detail in the Methods section.

In short, we plotted the relationship between the total number of sequences analyzed and the number of unique sequences detected (Figures 4b and 4c). The CPS of a primer set is represented as a black line on these plots, and red dashed lines indicate the CPS plus or minus one standard deviation. We then plotted phylogenetic trees from six previously published studies [8,9,14,17-19] as points on the same axes. Each plot in Figures 4b and 4c shows a different primer set, and each point represents a single phylogenetic tree generated using that primer set. Figure 4b shows results for trees composed of proviral DNA samples, and Figure 4c shows trees composed of plasma RNA samples. Trees containing both RNA and DNA were separated and evaluated individually; these trees are represented by separate points in Figure 4b and Figure 4c. The distance between the lines (CPS, background signal estimate) and the points (sample data) demonstrate the amount of true clonality likely to be present in a sample.

Figure 4. CPS of previously published amplicons. (**a**) CPS for each of the primer sets listed in Table 2, averaged over all subjects within each sample type (Table 1). (**b** and **c**) Evaluation of previously published phylogenetic trees in the context of the CPS of the primer sets used to generate those trees. Part **b** shows proviral DNA samples and part **c** shows plasma RNA samples. Black diagonal lines show the relationship between the number of sequences collected and the number expected to be unique for each primer set listed in Table 2, as an estimate of the background signal level (assuming no clonality); the slopes of these lines are equal to the CPS values in part a divided by 100. The dotted red lines were calculated as the black lines plus or minus one standard deviation in CPS. Each plotted point indicates the actual number of total sequences and unique sequences present in a previously published phylogenetic tree. Phylogenetic trees containing both proviral DNA and plasma RNA sequences were counted separately for the two sequence types and plotted separately in parts **b** and **c**. Points plotted far below the black line (green-shaded region) indicate trees with more clonality than would be expected by chance from a sample of unique HIV-1 genomes. **References in which hypermutated sequences were not explicitly included in phylogenetic trees.*

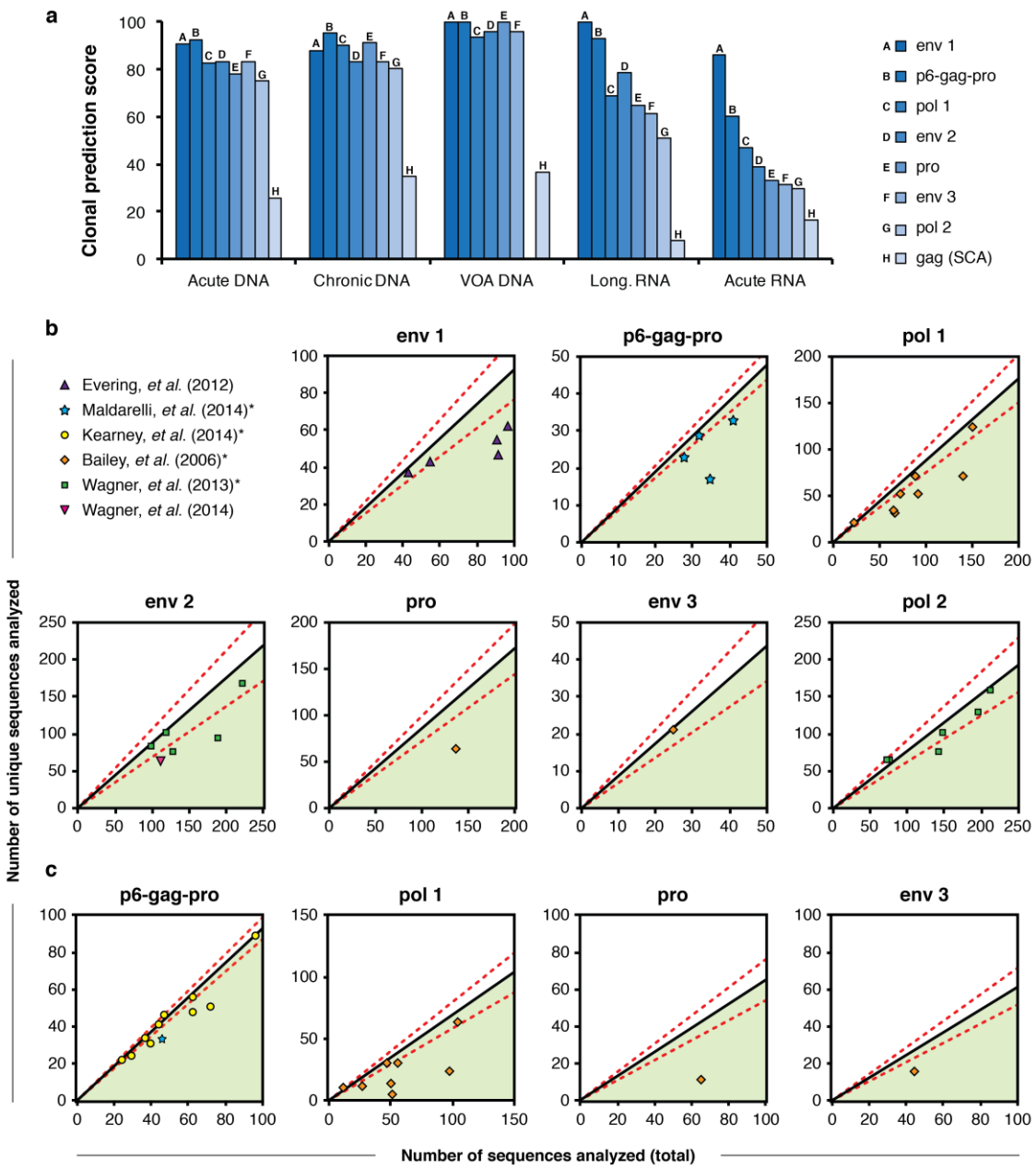
a
Clonal prediction score
Acute DNA
Chronic DNA
VOA DNA
Long. RNA
Acute RNA
A env 1
B p6-gag-pro
C pol 1
D env 2
E pro
F env 3
G pol 2
H gag (SCA)
b
Evering, et al. (2012)
Maldarelli, et al. (2014)*
Kearney, et al. (2014)*
Bailey, et al. (2006)*
Wagner, et al. (2013)*
Wagner, et al. (2014)
env 1
p6-gag-pro
pol 1
env 2
pro
env 3
pol 2
Number of unique sequences analyzed
c
p6-gag-pro
pol 1
pro
env 3
Number of sequences analyzed (total)

Importantly, the black lines in Figures 4b and 4c do not lie along the x=y axis. For every primer set defining a subgenomic amplicon, even in a sample composed entirely of unique HIV-1 genomes, some false-positive clonal amplicons are likely to be detected, causing the slope of the black line to deviate from 1. The expected number of false positive identical amplicons (y-axis) increases proportionally with the total number of amplicons sequenced (x-axis).

Points that lie on the black lines are consistent with the null hypothesis that there are no clonally expanded HIV-1 genomes in the sample. Points that fall below the black line suggest clonal expansion, *i.e.*, the presence of more identical amplicons than would be expected in a sample composed of unique viral genomes. We did not see evidence of points plotted well above the black line, which would have indicated greater sequence diversity than was present in the alignments used to generate this model. This observation serves as validation of the data sets used to train our model.

Studies in which trees do not include hypermutated sequences are marked with an asterisk. Hypermutated sequences are easily distinguishable even using short amplicons because of their tremendous diversity (Figure 8). For this reason, the removal of hypermutated or otherwise defective sequences from an alignment will artificially deflate the ratio of unique sequences to total sequences detected. In other words, for trees that have been curated to remove hypermutated sequences, the true location of the points plotted in Figures 4b and 4c is expected to fall closer to the black line. Due to the mechanisms of APOBEC-mediated hypermutation and HIV-1 reverse transcription, the rate of hypermutation is not constant across the viral genome[25,26]; the relationship between CPS and genome location in hypermutated sequences is shown in Figure 8b.

The analysis shown in Figure 4 provides a method for evaluating both primer sets and sequence data. A primer set with high CPS and minimal variation in CPS across samples provides the most powerful background estimate to enable the confident interpretation of sequence data. And regardless of the

primers used to generate sequences, phylogenetic trees and sequence alignments can only be understood properly when interpreted in the context of the CPS for the primer set used to generate them.

Discussion

In this study, we defined the CPS as a metric for how well a subgenomic amplicon differentiates unique HIV-1 genomes. We calculated CPS values for hypothetical amplicons of varying sizes across the HIV-1 genome to investigate the contribution of size and location to the capacity of an amplicon to distinguish unique genomes. Finally, we calculated the CPS values for commonly used primer sets and used them to estimate the background level of clonality in phylogenetic trees generated with those primer sets.

The primary goal of this study was to identify PCR amplicon(s) best suited to differentiate unique, full-length HIV-1 genomes. We found compelling evidence that no single, subgenomic amplicon will be sufficient to distinguish HIV-1 genomes across a variety of sample types or subjects. However, we evaluated eight previously published primer sets and found that of those, a 1.5 kb amplicon in the p6-gag-pro region seems to be the best compromise between coverage, practicality, and CPS, a metric which describes the capacity of an amplicon to correctly identify unique sequences as unique.

We also identified a variety of best practices to maximize the validity of future studies of HIV-1 clonality in any sample type. Most importantly, researchers should always emphasize which region is being sequenced and explicitly consider the CPS of the amplicon(s) used. This context is essential for evaluating claims of clonal expansion, as it provides an estimate of the expected background signal against which sequencing results should be compared. We recommend against highlighting identical amplicons as evidence of full-genome clonality without comparing those results to an appropriate

background estimate, and we emphasize that the only way to definitively demonstrate clonal expansion is to corroborate results with full-genome and integration site sequencing.

Importantly, all of the analyses presented here assume that the individual amplicons sequenced were collected independently using methods specifically designed for single-genome sequencing. Many studies are confounded by PCR resampling [28]; all sequences analyzed using the methods described here should be collected independently.

Furthermore, although some analyses call for curated sequence data, every full, uncurated data set should be made available. Phylogenetic trees presented to highlight clonally expanded populations should not be curated to remove replication-incompetent sequences. As described above, the removal of hypermutated sequences from a data set artificially inflates the proportion of clonal sequences in that data set. When evaluating alignments or trees against the background CPS of the amplicon sequenced, it is necessary to analyze every sequence collected.

To aid researchers in the analysis of new data sets with different amplicons than those described here, we have published a Web tool available at http://silicianolab.johnshopkins.edu/cps. This tool computes the CPS for user-specified primer sets and performs a comparison with user-entered values to characterize phylogenetic trees or alignments of amplicons in the context of appropriate background signal estimates.

Whether using this CPS analysis or any other method, it is impossible to conclusively prove or disprove the clonality of full-length viral genomes using only the sequence of a subgenomic amplicon. However, because information about the region amplified is available, it is essential to consider this context when interpreting data. These implications are no less relevant for phylogenetic studies in fields beyond HIV persistence; whenever the results and interpretation of a phylogenetic analysis may be

impacted by the choice of amplicon sequenced, it is critical to consider that impact explicitly in the evaluation and presentation of data. This CPS analysis is intended not as a definitive arbiter of full-sequence clonality but as a tool to quantify the context provided by primer location and inform the interpretation of sequence data.

Some important limitations of this study suggest additional considerations for future research. We have considered amplicon sequences on a binary scale; either sequences are correctly identified as unique, or they are not. We have not considered the distribution of sequence clonality. For example, in an amplicon alignment with twenty total sequences and only ten sequences correctly identified as unique, we did not distinguish between cases where the ten clonal sequences are identical to each other and cases where they represent duplicates of several other sequences. The case where all clonal sequences are identical may or may not be more likely to represent full-genome clonality; the quantification of that likelihood is beyond the scope of this study.

In this study, we took advantage of sequence alignments representing a variety of sample types. Importantly, the results of our analyses often varied dramatically, especially between plasma RNA HIV-1 genomes, which are typically intact, and proviral DNA genomes, which often contain large internal deletions. Although the CPS of a primer set is clearly correlated across sample types, the implications of our analysis for different sample types than those evaluated in this study are imprecise. We have also shown that even within a sample type, the variation in CPS among subjects can be extreme. Additionally, especially in the case of proviral DNA sequences containing deletions, the methods used to identify full-length genomic HIV-1 sequences in previous studies may have been more efficient for some sequences than for others. Any bias in the nature of the sequences used to define our CPS model may be reflected in our results. For these reasons, the model presented here and any future calculations of CPS would benefit from the inclusion of more full-length or near-full-length HIV-1 genome sequences and sample types collected in the future.

In summary, identical HIV-1 sequence fragments must be validated to demonstrate full-genome clonality conclusively. This validation can be achieved in a variety of ways. When technical constraints permit, additional regions of the genome can be sequenced. To demonstrate the clonality of proviral DNA sequences, the best validation is to sequence the associated integration site. Unvalidated sequences may be described as "identical throughout the region sequenced" but without further corroboration should not be described as clonally expanded. The web tool available at http://silicianolab.johnshopkins.edu/cps can be used to calculate CPS for the evaluation of new data or primer sets not described in this study.

Methods

Online tool. The online tool to calculate CPS can be found at http://silicianolab.johnshopkins.edu/cps. The tool is written in JavaScript, and the code is accessible at https://github.com/gitliver/HIVCPS. All sequences used for CPS analysis are available from GenBank.

CPS plots. The CPS values in Figure 4a are similar across all three DNA sample types. To calculate the expected CPS of a given primer set as used to characterize a proviral DNA sample, we averaged the CPS of that primer set for the three DNA sample types. To calculate the expected CPS of a given primer set used to characterize a plasma RNA sample, we used the average CPS from the Longitudinal – RNA samples (Figure 4a). We chose not to include the Acute – RNA samples in this average because plasma virus from acutely infected individuals contains much less diversity than any other sample type, and its relevance to the analysis of other samples is minimal. The appearance of the Acute – RNA sample type as an outlier is evident in Figures 1, 2, and 4a.

For each primer set in Table 2, we used the average CPS values for proviral DNA and plasma RNA samples to calculate the proportion of false-positive clonal sequences that should be expected from sequencing subgenomic HIV-1 RNA or DNA amplicons. The relationship between the total number of amplicons sequenced and the expected number of correctly identified unique amplicons detected for each primer set is plotted as a black line in Figures 4b (proviral DNA) and 4c (plasma RNA). The slope of this line is the CPS divided by 100. The dashed red lines give a confidence interval representing one standard deviation in CPS values.

We counted the total number of sequences and the number of unique sequences in 53 different phylogenetic trees from six previously published studies [8,9,14,17-19]. The color and shape of the points indicate the study in which each tree was published.

Acknowledgments

Many thanks to Oliver Elliott for adapting the CPS calculator algorithm into an online tool. The authors would also like to thank Dr. Christine Durand, Dr. Andrew Redd, Dr. Stuart Ray, and Dr. Daniel Rosenbloom for helpful discussions and advice.

The work presented in this chapter is in press as of this writing [30].

Supplementary Material

Table 3. Number and subtype of unique sequences analyzed for each subject.

Sample/Subject	Unique sequences analyzed	HIV subtype
Acute treated – DNA		
2286	12	B
2443	8	B
2453	7	B
2521	14	B
2529	7	B
3693	12	B
Chronic treated – DNA		
CP02	10	B
CP03	8	B
CP06	8	B
CP07	9	B
CP10	13	B
VOA – DNA		
VOA10	12	B
VOA16	10	B
VOA17	6	C
VOA20	9	B
VOA22	7	B
Longitudinal – RNA		
PIC11286	28	B
PIC38417	92	B
PIC55751	37	B
PIC71101	80	B
PIC83747	121	B
PIC90770	67	B
Acute – RNA		
226_2	9	B
CH40	6	B
CH58	7	B
CH77	5	B
TRJO	5	B
WEAU	7	B
WITO	14	B
ZM247F(A)	5	C
ZM249M	6	C

Figure 5. Clonal prediction scores are equivalent for different, equally probable alignments of the same sequences. The Longitudinal – RNA sample sequences were aligned to the HXB2 reference genome in two different but equally probable alignments. CPS values were calculated for 1 kb amplicons spanning the viral genome at 10 bp intervals (see Figure 1). Parts a and b show that CPS values are equivalent for the two different alignments.

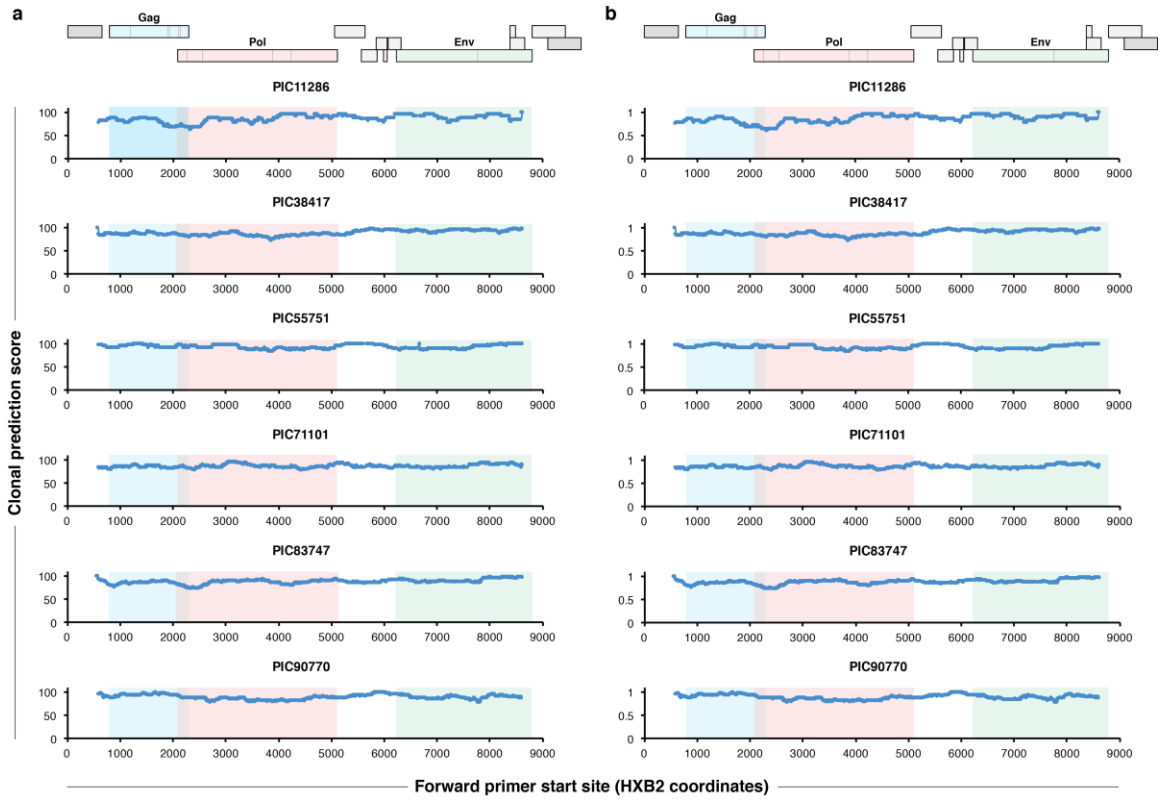

Figure 6. Clonal prediction scores of hypothetical amplicons are insensitive to the choice of hypothetical primer length. CPS values were calculated for 1 kb amplicons spanning the viral genome at 10 bp intervals. These amplicons were defined by hypothetical primers based on the HXB2 reference genome. The choice of hypothetical primer length used to define the amplicons characterized in Figure 1 is arbitrary; we show here that the results in Figure 1d are insensitive to variation in hypothetical primer length.

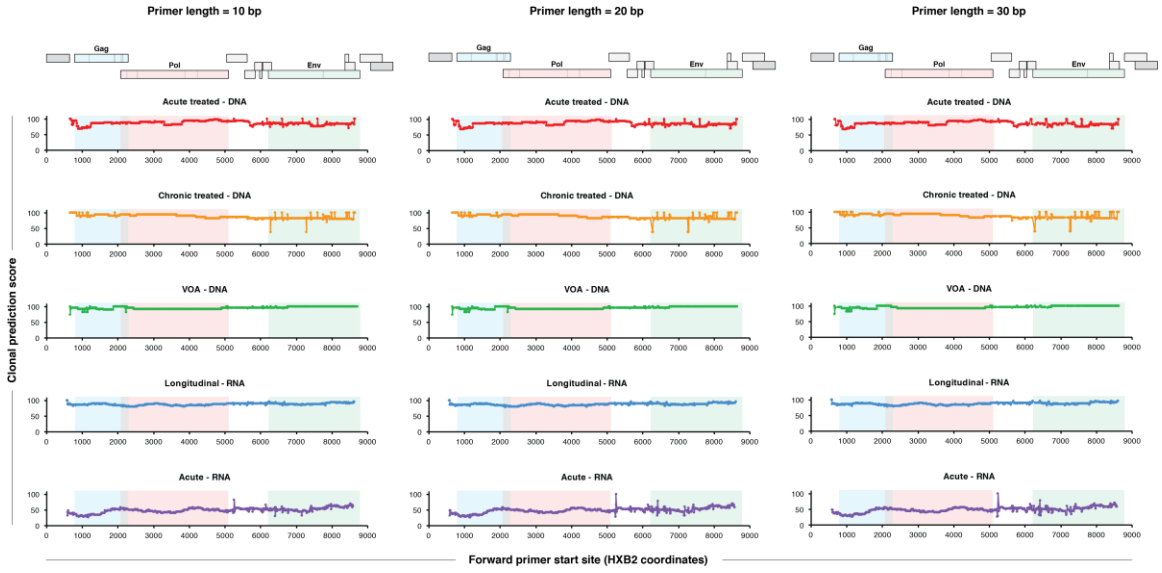

Figure 7. Clonal prediction scores of 1 kb amplicons spanning the HIV-1 genome for individual subject sequence alignments. CPS of 1 kb-wide amplicons spanning the HIV-1 genome for all subjects not shown in Figure 1b. The average of these plots over all subjects within each sample type are shown in Figure 1c.

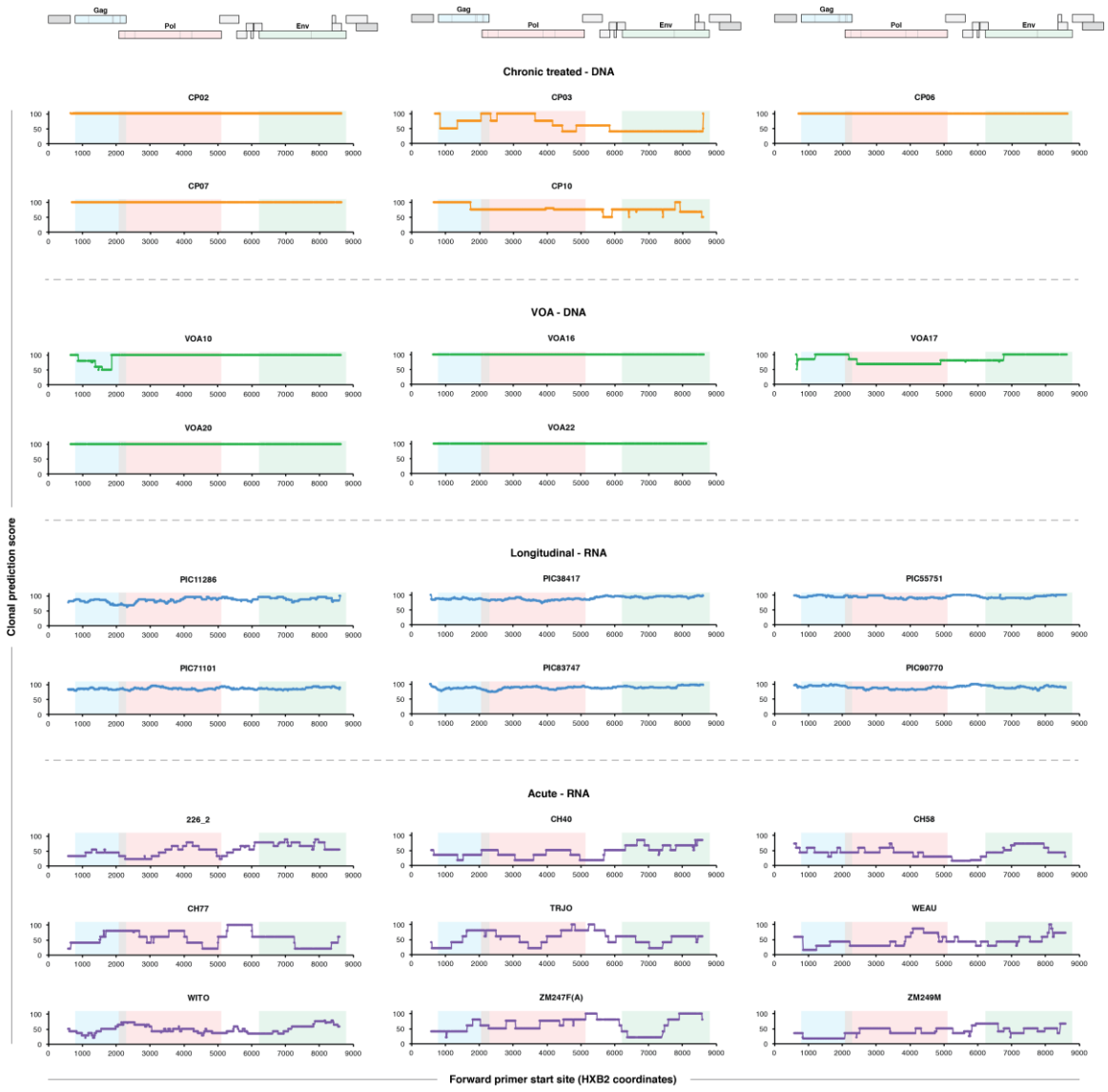

Figure 8. Clonal prediction scores of hypothetical short amplicons used to characterize hypermutated or non-hypermutated sequences. CPS values were calculated separately for the hypermutated and non-hypermutated sequences from the same subjects. Results are shown for four subjects with ≥4 unique hypermutated sequences and ≥3 unique non-hypermutated sequences. (**a**) Average CPS values over all hypothetical amplicons of a given length spanning the viral genome are shown for the hypermutated-only and non-hypermutated-only alignments (see Figure 2). CPS values are higher for hypermutated sequences, indicating that hypermutated sequences are much easier to distinguish than non-hypermutated sequences using amplicons as small as 100 bp. (**b**) CPS of 200 bp-wide amplicons spanning the HIV-1 genome (see Figure 1) with hypermutated and non-hypermutated sequences evaluated separately. The top plot emphasizes locations in the genome where even hypermutated sequences are not always distinguishable by a 200 bp amplicon.

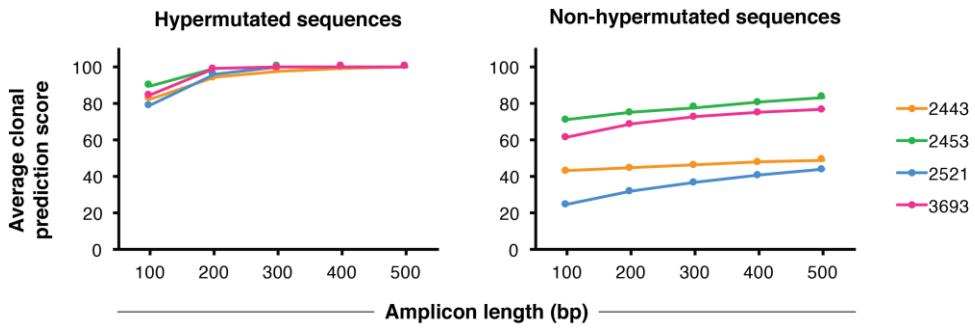

Chapter II: A Quantitative Basis for the Clinical Success of Dolutegravir

Abstract

The clinical success of antiretroviral drugs against HIV-1 is highly correlated with the results of *in vitro* assays that quantify drug efficacy. The only exceptions are the first-generation integrase strand transfer inhibitors (InSTIs), which are under-valued by *in vitro* models. The second-generation InSTI dolutegravir (DTG), which has been in clinical use since late 2013, has not been described using these analyses. To develop a quantitative understanding of its efficacy and mechanism of action, we evaluated DTG using quantitative *in vitro* infectivity assays. We measured the efficacy of DTG alone and in combination with nucleoside reverse transcriptase inhibitors (NRTIs), and we measured the ability of DTG to inhibit both wild-type HIV-1 and virus containing InSTI resistance mutations. The results of our analysis were consistent with the clinical success of DTG. We demonstrated a high genetic barrier to DTG resistance; favorable interactions between DTG and NRTIs; and a mechanism of action for DTG consistent with that of the successful first-generation InSTI raltegravir. We showed that the recommended DTG-based regimens for treatment of HIV-1 are sufficiently efficacious to inhibit all viral replication at clinical concentrations, suggesting that this second-generation InSTI is not under-valued by our quantitative *in vitro* model of antiretroviral drug efficacy.

Introduction

Two years after its approval, the second-generation HIV-1 integrase strand transfer inhibitor (InSTI) dolutegravir (DTG) has demonstrated not only efficacy [31-35] but also cost-effectiveness [36] and a high barrier to resistance *in vivo* [37,38]. Despite the remarkable clinical success of DTG, its pharmacodynamic properties in combination with other antiretroviral drugs and against HIV-1 containing InSTI resistance mutations have not been evaluated comprehensively using quantitative *in*

vitro models. Despite underestimating the efficacy of first-generation InSTIs, the results of these models correlate closely with the clinical success of antiretroviral drug regimens used to treat HIV-1 [39,40].

A quantitative understanding of antiretroviral efficacy allows for a more thorough theoretical evaluation of antiretroviral therapy than is feasible in a clinical setting. The extensive variety of available drugs, along with their typically combinatorial usage, yields far more possible drug combinations than can be practically tested individually in the clinic. Moreover, determination of the parameters that define a dose-response relationship allows for the extrapolation of drug efficacy at very high, clinical concentrations, which are beyond the detection range of *in vitro* assays. Quantitative analyses describing the efficacies of antiretroviral drugs can be used to predict more efficacious drug regimens, both for wide clinical use and for salvage therapy in the case of multi-drug resistant virus.

We used an *in vitro* infectivity assay and subsequent quantitative modeling to evaluate the efficacy of DTG in combination with nucleoside analog reverse transcriptase inhibitor (NRTI) pairs abacavir/lamivudine (ABC/3TC) and tenofovir/emtricitabine (TDF/FTC). To quantify the genetic barrier to DTG resistance, we measured pharmacodynamic properties of DTG against HIV-1 containing InSTI resistance mutations. We also hypothesized that the excellent clinical efficacy of dolutegravir might be due to inhibition of integration as well as late steps in the HIV-1 life cycle, which are not measured by standard infectivity assays [39,40]. This hypothesis is suggested by the finding that allosteric integrase inhibitors (ALLINIs) affect HIV-1 maturation as well as integration [41-45]. The first-generation InSTI raltegravir has not shown activity at posttranslational steps of the HIV-1 life cycle [41-43], but the efficacy of dolutegravir against these steps has not been assessed.

Results and Discussion

DTG interacts favorably with NRTIs. We measured the dose-response relationships for DTG, ABC, 3TC, TDF, and FTC separately and in combination using a phenotypic assay that quantifies the number of single-round infection events inhibited by a given concentration of one or more drugs (see Methods). The median effect curves plotted in Figure 9A show the log of drug concentration plotted against a logarithmic metric of efficacy; curves are linear for drugs that act without cooperativity [39]. The three-drug combinations shown (ABC/3TC/DTG and TDF/FTC/DTG) are DHHS-recommended treatment regimens for individuals initiating antiretroviral therapy [46].

We used the Loewe additivity [47] and Bliss independence [48] models of combined drug efficacy to calculate the expected efficacies of drug combinations given the experimentally determined efficacies of the individual component drugs. Loewe additivity assumes that drugs act through the same target; Bliss independence describes drugs that inhibit distinct targets. At clinically relevant concentrations, the Loewe model predicts lower combined efficacy than the Bliss model. Importantly, in practice, antiretroviral drugs do not interact exclusively according to either model; understanding how drugs interact with reference to these models allows the prediction of combined efficacy at concentrations beyond the limits of *in vitro* assays, including clinical concentrations [40].

In Figure 9A, the interactions between drugs can be quantified by comparing the drug combination dose-response curves (gray) to the Loewe (red dashed) and Bliss (blue dashed) model predictions. Degree of independence (DI), a scale defined by the Loewe and Bliss models, describes these interactions quantitatively. Some antiretroviral drug combinations exhibit an intermediate DI with efficacy between the Loewe and Bliss predictions, and other combinations exhibit synergy, defined as a higher combined efficacy than that predicted by the Bliss model [40]. Pie charts in Figure 9A show DI

Figure 9. Efficacy of DTG and NRTIs alone and in combination. (**A**) Median effect curves, with normalized logarithmic drug concentration (x-axis) plotted against a logarithmic measure of efficacy (y-axis). f_a is the fraction of infection events affected, *i.e.* inhibited, by the drug(s) at the stated concentration; f_u is the fraction of infection events unaffected by the drug(s), and $f_u = 1 - f_a$. Solid lines show experimentally determined dose-response relationships, with the color distinguishing the drug(s) used. The gray "combination" line refers to the combination specified in the label above each chart. Dashed lines show the Loewe additivity (red) and Bliss independence (blue) model predictions for combined efficacy given the experimentally determined efficacies of the individual drugs. Drug concentrations were chosen so that all drugs would have similar efficacy at the reference concentration D_0: $[D_{0,DTG}]$=52.7nM; $[D_{0,ABC}]$=558nM; $[D_{0,3TC}]$=434nM; $[D_{0,TDF}]$=354nM; $[D_{0,FTC}]$=110nM. Error bars show the standard deviation of six biological replicates. Inset pie charts show degree of independence (DI) calculated for two- and three-drug combinations, according to the color scale in the legend, based on the empirically determined dose-response relationships. Each pie slice shows the results from a different biological replicate. (**B**) Average IIP over a 24-hour dosing period for individual drugs and their combinations. A dashed line at IIP=5 shows the minimum IIP for a fully suppressive antiretroviral regimen.

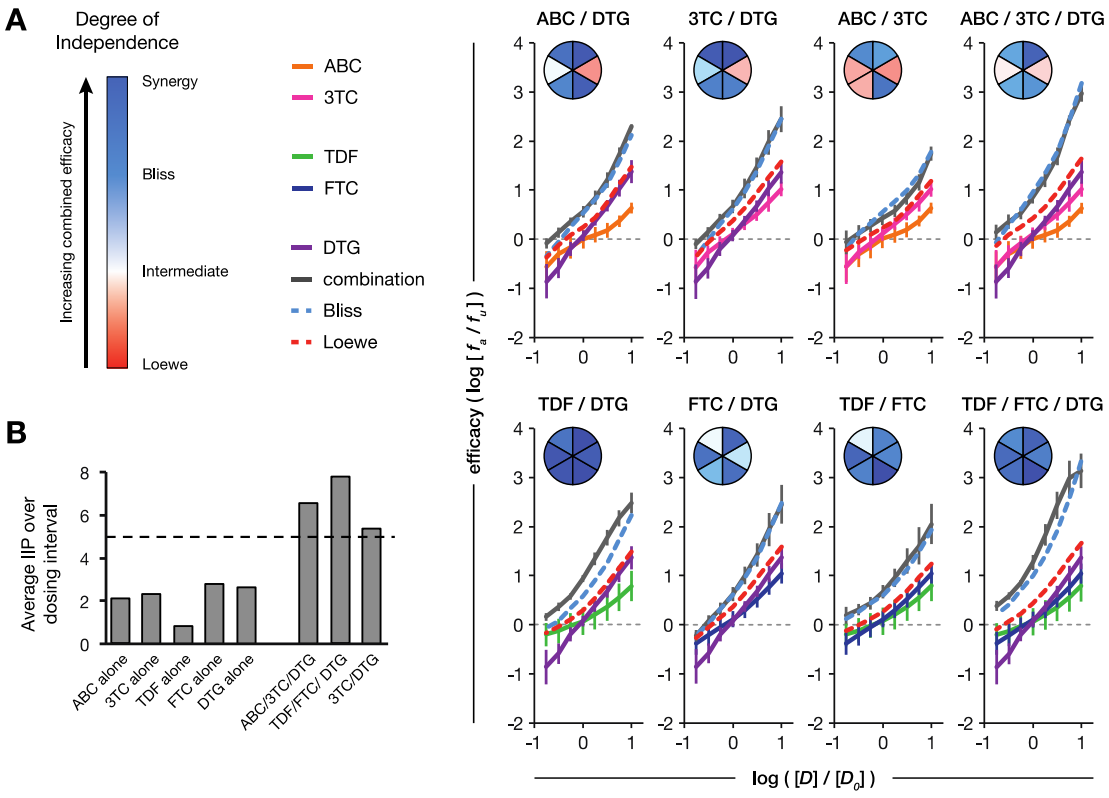
A
Degree of Independence
Increasing combined efficacy
Synergy
Bliss
Intermediate
Loewe
ABC
3TC
TDF
FTC
DTG
combination
Bliss
Loewe
B
Average IIP over dosing interval
ABC alone
3TC alone
TDF alone
FTC alone
DTG alone
ABC/3TC/DTG
TDF/FTC/ DTG
3TC/DTG
ABC / DTG
3TC / DTG
ABC / 3TC
ABC / 3TC / DTG
TDF / DTG
FTC / DTG
TDF / FTC
TDF / FTC / DTG
efficacy (log [f_a / f_u])
log ([D] / [D_0])

values for DTG combined with NRTI(s). There is some variation among donors; overall, DTG/ABC/3TC interact according to the Bliss model, and DTG/TDF/FTC interact synergistically.

DTG-based regimens have sufficient efficacy to suppress viremia. Instantaneous inhibitory potential (IIP) quantifies the number of logs by which HIV-1 infection is reduced by a drug or drug combination [39]. IIP is a function of the drug concentration(s) as well as the slope and IC_{50} parameters that describe dose-response curve(s), and the IIP for a drug combination depends on the DI of the combination. Regimens with a combined average IIP>5 throughout the dosing interval typically are able to control HIV-1 infection completely in a clinical context [40]. Figure 9B shows average IIP over the dosing interval for individual drugs and the three-drug combinations DTG/ABC/3TC and DTG/TDF/FTC, as well as the two-drug combination DTG/3TC, which has shown some clinical efficacy [49]. For all three combinations, the average IIP over the dosing interval is >5, consistent with complete viral suppression in a clinical context.

DTG has a high genetic barrier to resistance. We tested the ability of DTG to inhibit HIV-1 containing previously characterized InSTI resistance mutations. Figure 10A shows median effect dose-response curves for DTG against a panel of drug-resistant viruses. The high genetic barrier to DTG resistance is evident from the modest effect of resistance mutations on the IC_{50} of DTG (Figure10); the impact of these resistance mutations on first-generation InSTI IC_{50}—and of canonical drug resistance mutations for other antiretroviral drug classes—is often orders of magnitude higher [50]. Additionally, although drug resistance mutations have been shown to dramatically impact the slope of the dose-response curves for antiretroviral drugs from other classes, the slopes of first-generation InSTIs are relatively constant even in the context of drug-resistant virus [50]. DTG recapitulates this phenotype, as all of the median effect curves in Figure 10A have similar slopes (Figure 10C).

Figure 10. Pharmacodynamic properties of DTG against HIV-1 containing InSTI resistance mutations. (**A**) Median effect dose-response curves showing DTG efficacy against various drug-resistant viruses. For this plot, the reference concentration [DTG_0]=50nM. (**B**) Fold change in IC_{50} of DTG dose-response curves for drug-resistant viruses as compared to wild-type virus. (**C**) Fractional change in slope of DTG dose-response curves for drug-resistant viruses as compared to wild-type virus. (**D**) IIP of DTG at the maximal clinical concentration(C_{max}) against wild-type and drug-resistant viruses. IIP is a function of the IC_{50}, the dose-response curve slope, and the drug concentration. (**E**) Fractional change in IIP of DTG at C_{max} against drug-resistant viruses as compared to wild-type viruses. (**F**) Replication capacity of wild-type and drug-resistant viruses, measured as the ratio of maximal infection levels in culture for drug-resistant and wild-type virus. (**G**) Selective advantage of each virus at C_{max}. Selective advantage is defined as the replication capacity of the drug-resistant virus multiplied by the ratio of the infectivity for the drug-resistant virus to the infectivity for the wild-type virus, where infectivity is defined as the proportion of infection events unaffected by the drug, or f_u [50].

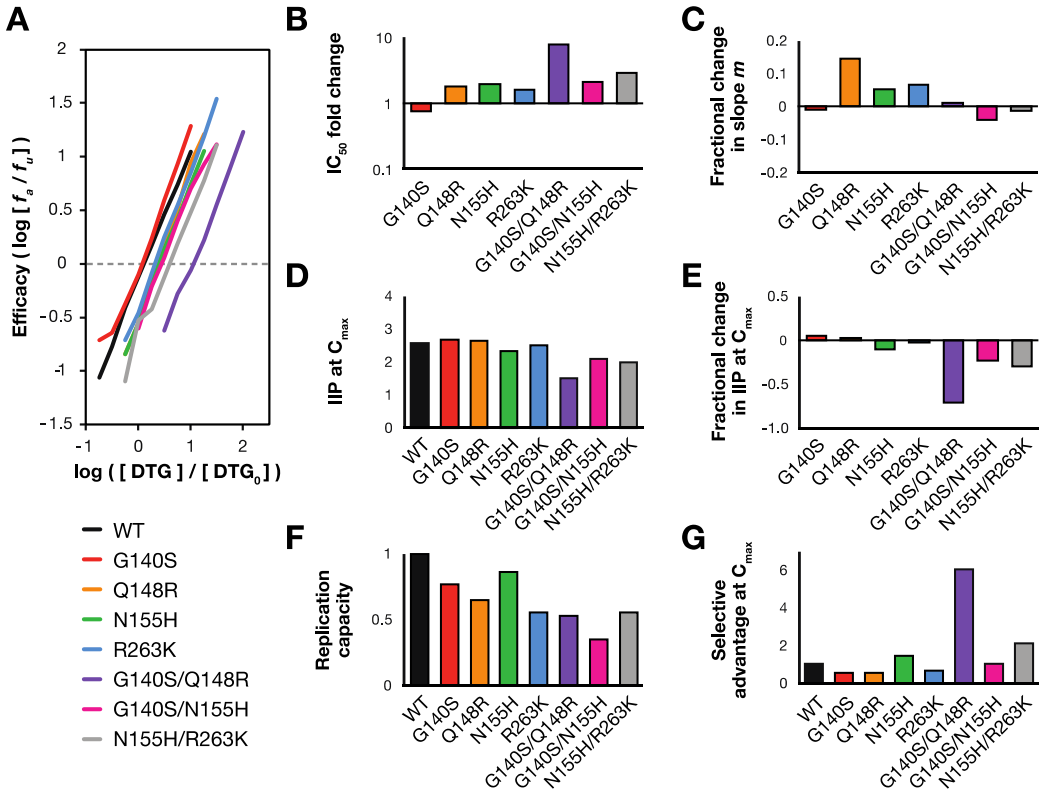

The combined impact of drug resistance mutations on DTG efficacy can be demonstrated by IIP, which takes into account the effect of resistance mutations on dose-response curve slope and IC_{50}. The impact of resistance mutations on the IIP of DTG at the maximum clinical concentration (C_{max}) is shown in Figures 10D and 10E. Single point mutations have minimal impact on the IIP of DTG, and the change in IIP due to combinations of two point mutations is of comparable magnitude to that of single point mutations in first-generation InSTIs and other drug classes [50].

The ability of a drug-resistant virus to replicate in the presence of the drug is impacted both by the magnitude of resistance conferred by a mutation and by the fitness cost of that mutation. The impact on viral fitness of the InSTI resistance mutations tested is shown in Figure 10F. The selective advantage of each viral strain, which takes into account both the magnitude of resistance and the fitness cost of resistance, is shown in Figure 10G. The virus with the greatest replicative advantage over wild-type is G140S/Q148R, which combines a ten-fold shift in IC_{50} with only a moderate fitness cost. The G140S mutation, which confers no resistance on its own, has been shown to act as a compensatory mutation for other InSTI resistance mutants [51].

DTG does not act late in the HIV-1 life cycle. To determine whether the success of DTG is due in part to activity during late steps of the HIV-1 life cycle (virus assembly, release, and maturation), we designed a modified phenotypic assay (Figure 11A, Methods). Maximally activated $CD4^+$ T cells were infected with two different viral inoculums, which contained equal concentrations of drug and virus; the only difference between the conditions was whether the virus was produced and consequently underwent the posttranslational steps of the HIV-1 life cycle in the presence (Inoculum A) or absence (Inoculum B) of integrase inhibitors. We used the first-generation InSTI raltegravir as a negative control for late life cycle activity [41-43] and the ALLINI BI-D, which has been shown to inhibit virion maturation, as a positive control [41-45].

Figure 11. Activity of integrase inhibitors in early and late portions of HIV-1 life cycle. (**A**) Schematic of inoculum preparation for the life cycle assay, which differentiates between virus activity early and late in the HIV-1 life cycle. Virus is produced either in the presence or the absence of a drug and then drug/virus combinations are used to infect primary $CD4^+$ T cells. (**B**) Median effect dose-response curves for BI-D (left), raltegravir (center), and dolutegravir (right). Open circles represent data points below the detection range of the assay. The top row shows the individual results from five healthy blood donors; error bars represent the standard deviation of three technical replicates. The bottom row shows the results averaged over all five biological replicates in each condition, with error bars representing one standard deviation. Due to the design of this assay, drugs are at 20-fold higher concentration during the virus preparation step than during the infection step; reference concentrations refer to the drug concentration during virus production. Reference concentrations for these plots are: $[D_{0,DTG}]$=45nM; $[D_{0,RAL}]$=97nM; $[D_{0,BI\text{-}D}]$=50 nM.

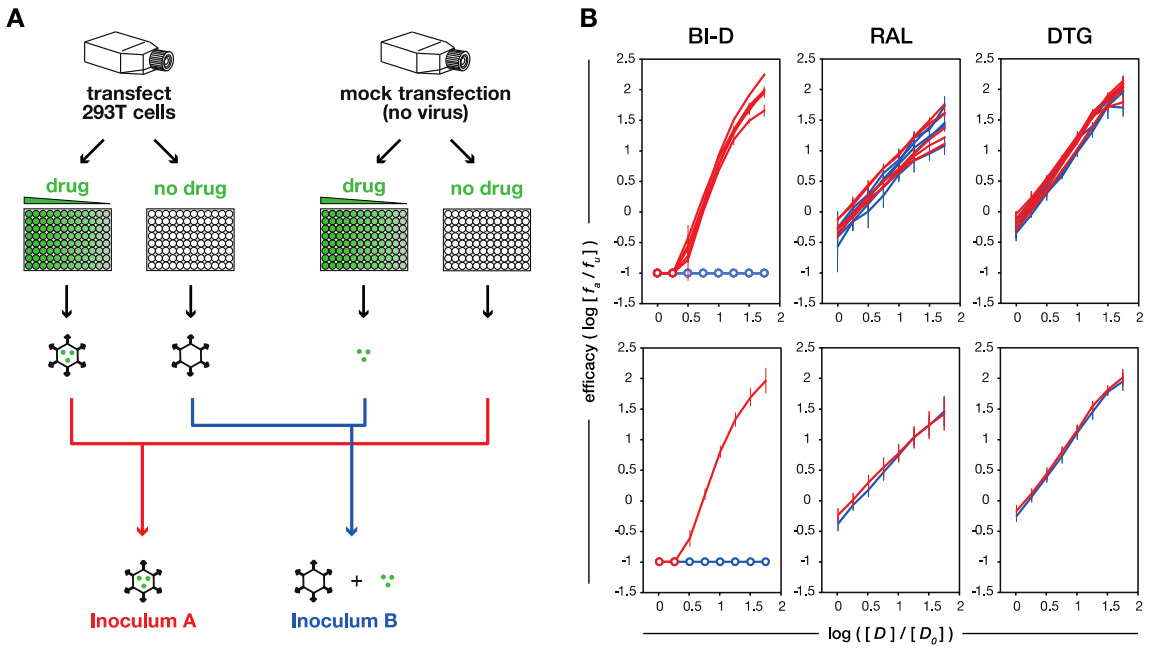

The difference between virus produced in the presence versus the absence of BI-D is dramatic, with a >2.5-log difference in inhibition at the highest concentration tested (Figure 11B, left). Although inhibition of infection by BI-D present during virion maturation (Inoculum A) was readily detected, infection was not inhibited by BI-D that was combined with virus after the completion of maturation (Inoculum B) at any concentration tested. This is consistent with a previous report that the IC_{50} of BI-D as an integrase inhibitor is 13-fold higher than the IC_{50} of BI-D as a maturation inhibitor [44]. In sharp contrast to the results obtained with BI-D, there was no difference in infectivity between virus produced in the presence or the absence of raltegravir, with <0.2-log difference in inhibition between Inoculums A and B at all concentrations tested (Figure 11A, center). These contrasting results for raltegravir and BI-D demonstrate the ability of our assay to measure drug effects on late steps in the HIV-1 life cycle separately from effects on integration.

Figure 11A (right) shows median effect dose-response curves for DTG. There is no difference in infectivity between virus produced in the presence of DTG and virus produced without drug. High dose-response curve slopes and nonlinear dose-response curves are indicative of antiretroviral drugs that act at multiple steps of the HIV-1 life cycle [52], and high slopes correspond with high *in vitro* efficacy at clinical concentrations [39,40,52]. Both Inoculums A and B have DTG dose-response curves with slopes of 1.3 ± 0.1, consistently higher than the slope of ~1 previously reported for first-generation InSTIs [39].

Conclusions. The overwhelming clinical success and rapidly increasing popularity of DTG suggest the importance of extending the quantitative framework describing antiretroviral therapy [39,40,50,53] to include this second-generation InSTI. DTG shares many pharmacodynamic features with first-generation InSTIs, including efficacy restricted to the early part of the HIV-1 life cycle and a linear median-effect dose-response curve with a slope that remains consistent despite resistance mutations. However, DTG has a higher dose-response curve slope than first-generation InSTIs, which translates to higher predicted efficacy at clinical concentrations. Importantly, this quantitative model, which has

been shown to undervalue first-generation InSTIs, predicts sufficient efficacy at clinical concentrations to completely suppress viremia for both ABC/3TC/DTG and TDF/FTC/DTG, consistent with the clinical success of these two regimens. This high efficacy is due to both the steeper slope of DTG and the favorable interactions between DTG and the NRTIs.

Methods

Phenotypic assay. The phenotypic assay used to quantify DTG efficacy alone and in combination against WT and mutant HIV-1 has been previously described [29,30,50,54]. Briefly, maximally activated primary $CD4^+$ T lymphoblasts from healthy blood donors were spinoculated with the single-round fluorescent reporter virus NL4-3 ΔEnv-EGFP in the presence of varying concentrations of drug(s), and the proportion of infected cells was quantified by FACS.

Life cycle assay. 293T cells were transfected using Lipofectamine 2000 (Life Technologies) with a plasmid carrying the proviral clone NL4-3 with EGFP in place of the *env* gene and a separate plasmid carrying the IIIB *env* gene to produce single-round fluorescent reporter virus. A second flask of 293T cells was mock transfected. 6-7 hours after transfection, the cells were trypsinized and transferred to 96-well plates in media comprised of 45% RPMI, 5% FBS, 50% human serum (Gemini), and 12mM HEPES. Integrase inhibitors were added to half of the wells to produce the following conditions: 1) transfected 293T cells incubated with drug, 2) transfected 293T cells incubated without drug, 3) mock transfected 293T cells incubated with drug, and 4) mock transfected 293T cells incubated without drug (Figure 11A).

After a 48-hour incubation, supernatant was recovered, centrifuged briefly to remove cellular debris, and transferred to a fresh plate. The conditions described above produced supernatant containing the following: 1) virus matured in the presence of drug, 2) virus matured in the absence of drug, 3) drug

without virus, and 4) neither virus nor drug. Supernatants 1 and 4 were combined at equal volumes to yield *Inoculum A*, virus produced in the presence of drug. Supernatants 2 and 3 were combined at equal volumes to yield *Inoculum B*, virus and drug that had been incubated separately. Both combinations were used to infect PHA-activated primary $CD4^+$ T lymphoblasts by spinoculation at 1200 x g and 37°C for two hours. Infection was measured after 72 hours by EGFP fluorescence on a FACSCalibur (BD).

Analysis. Previously published values were used for the slope, IC_{50}, C_{max}, and half-life parameters of ABC, 3TC, TDF, FTC [40], as well as the C_{max} and half-life of DTG [55]. The IIP for each drug combination according to the Loewe, Bliss, or empirical estimate of combined drug efficacy was calculated for every minute over a 24-hour dosing interval assuming rapid drug penetration. Average IIP over the dosing interval was reported as the average of these values. The average IIP calculation was performed using a python script, which is available upon request.

Discussion

Clonal expansion in the latent HIV reservoir

A full explication of my opinions on HIV latency research far exceeds the scope of this dissertation. Briefly, I am all but convinced that strategies intended to diminish the size of the latent HIV reservoir cannot and will not ever form the basis of a successful HIV cure. Among other considerations, this opinion is based in a quantitative understanding of data that I think are typically interpreted qualitatively. My greatest hope for the HIV cure field is that it manages to prove me wrong as swiftly as possible.

Toward that end, researchers in the field are studying the composition, establishment, and variation of the HIV reservoir in resting $CD4^+$ T cells. The analysis presented in Chapter I of this dissertation was intended to encourage reflection, attention to detail, and quantitative thinking, all of which should improve the quality and applicability of any biomedical research regardless of its ultimate practical use.

I initially developed the clonal prediction score metric to be a mirror, not a tool. My goal was to emphasize to researchers the obvious but infrequently acknowledged limitations of their assays and, ideally, encourage them to consider those limitations in the interpretation of results. We designed the online CPS calculator to facilitate that process, but it has severe limitations of its own. Most critically and least surprisingly, there just is not enough full-length HIV sequence data available to support the robust and precise calculation of CPS, especially for a variety of samples and sample types. The limitations of my resources are reflected in the deficiencies of my finished product, but I hope that the CPS calculator—much like the analysis of short, identical HIV sequence regions—can still provide practically useful, if technically inconclusive, data.

If the CPS calculator is never used, but some scientist somewhere is inspired by its theoretical basis to present results alongside an explicit discussion of their technical limitations, then I will be satisfied with the impact of the work presented here.

Quantifying the efficacy of antiretroviral therapy

To put it bluntly, the "context of related work in the literature"[1] for this project is as follows: The Siliciano lab published several papers establishing a quantitative framework to explain the efficacy of antiretroviral drugs. Other groups evidently saw these publications and read them; I have discussed their content with members of the federal government, other academic research institutions, and even pharmaceutical companies. Nevertheless, the work was met with a glaring lack of follow-up research or practical implementation by any other group, including those who so readily praised it. The ultimate implication of these premises is impossible to ignore; notwithstanding their pretty compliments, no one (myself and my advisor awkwardly excluded) was interested in seeing more work in this vein.

Knowing this, I chose to evaluate dolutegravir with the quantitative model anyway. While I really am pleased with the quality of the data I produced, the most realistic and perhaps rational future direction for this project is a dusty corner of Bernard Forscher's metaphorical brickyard[2]. Given its inauspicious foundation, I see little advantage to be gained by incorporating my brick into a wall.

While considering the limitations and future directions of projects including the one presented in Chapter II of this dissertation, I started to conceive of a fundamentally different but potentially informative framework for the quantitative evaluation of antiretroviral drugs. Much to the chagrin of

[1] Biomedical Engineering PhD Guidelines, Johns Hopkins School of Medicine, June 2015.
[2] Chaos in the Brickyard, Bernard K Forscher, *Science*, 1963.

my advisor, I am sure, this new model relies on the understanding that suppressive antiretroviral therapy may not entirely prevent new HIV infection events in the body of a treated patient. Rather, it may be the case that suppressive antiretroviral therapy prevents *new viral lineages of enough generations to evolve multi-drug resistance*—an important distinction which I will explain in more detail below.

To the extent that I am forced by lack of an alternative to believe published scientific results, I see no way to dispute the following:

1. The notable historical absence of drug resistance in patients adhering to suppressive antiretroviral treatment is far too robust to believe that substantial viral replication could take place in the presence of therapy, even if said replication were largely restricted to anatomical sanctuaries.
2. The consistent clinical evidence of increases in 2LTR circles upon raltegravir intensification of suppressive regimens is far too robust to believe that *all* viral replication is inhibited even by the most efficacious combination therapy.[3]

I am likewise convinced that these two statements are perfectly reconcilable. “When you have eliminated the impossible, whatever remains, *however improbable*, must be the truth.”[4]

In the face of these data, I am forced to conclude that some ongoing HIV replication takes place in the face of suppressive antiretroviral therapy, but that replication is insufficient to produce multi-drug resistant virus. My hypothesis relies on the vanishingly low probability of HIV evolving high-level

[3] Even if these findings are entirely restricted to patients receiving protease inhibitor-based regimens, a rebuttal based on that fact must assume that protease inhibitor-based regimens are not fully suppressive throughout the dosing period, and therefore that ongoing replication should be expected at least in patients treated with protease inhibitors.
[4] The Sign of the Four, Arthur Conan Doyle, *Lippincott’s Monthly* Magazine, 1890.

resistance to every component of a combination drug regimen during a single round of replication. Instead, the evolution of multi-drug resistance is much more likely to comprise the sequential accumulation of resistance mutations across several viral generations. A virus replicating with a small but nonzero reproductive ratio (R_0) might produce new infection events consistently without ever achieving the long viral lineages necessary to accumulate multiple resistance mutations. In this way, the ongoing replication implied by treatment intensification studies is compatible with the long-term viral suppression of treated individuals.

I think that an instructive framework for evaluating the efficacy of antiretroviral therapy might quantify the distribution of viral lineage lengths in the presence of drug(s), rather than the single-round inhibition of viral infection. Such a model would expect some ongoing replication in the presence of treatment without necessarily predicting the resultant evolution of multi-drug resistant virus.

References

1. World Health Organization. Progress Report – Global Health Sector Response to HIV, 2000-2015: Focus on Innovations in Africa. Available at http://apps.who.int/iris/bitstream/10665/198065/1/9789241509824_eng.pdf. Accessed May 13, 2016.
2. Chun T-W, Carruth L, Finzi D, Shen X, DiGiuseppe JA, Taylor H, et al. Quantification of latent tissue reservoirs and total body viral load in HIV-1 infection. Nature. 1997;387: 183–188. doi:10.1038/387183a0
3. Finzi D, Hermankova M, Pierson T, Carruth LM, Buck C, Chaisson RE, et al. Identification of a reservoir for HIV-1 in patients on highly active antiretroviral therapy. Science. 1997;278: 1295–300.
4. Wong JK, Hezareh M, Günthard HF, Havlir D V, Ignacio CC, Spina CA, et al. Recovery of replication-competent HIV despite prolonged suppression of plasma viremia. Science. 1997;278: 1291–5.
5. Finzi D, Blankson J, Siliciano JD, Margolick JB, Chadwick K, Pierson T, et al. Latent infection of CD4+ T cells provides a mechanism for lifelong persistence of HIV-1, even in patients on effective combination therapy. Nat Med. 1999;5: 512–7. doi:10.1038/8394
6. Ruelas DS, Greene WC. An Integrated Overview of HIV-1 Latency. Cell. 2013;155: 519–529. doi:10.1016/j.cell.2013.09.044
7. Bruner KM, Hosmane NN, Siliciano RF. Towards an HIV-1 cure: measuring the latent reservoir. Trends Microbiol. 2015;23: 192–203. doi:10.1016/j.tim.2015.01.013
8. Maldarelli F, Wu X, Su L, Simonetti FR, Shao W, Hill S, et al. Specific HIV integration sites are linked to clonal expansion and persistence of infected cells. Science. 2014;345: 179–183. doi:10.1126/science.1254194
9. Wagner TA, McLaughlin S, Garg K, Cheung CYK, Larsen BB, Styrchak S, et al. HIV latency. Proliferation of cells with HIV integrated into cancer genes contributes to persistent infection. Science. 2014;345: 570–3. doi:10.1126/science.1256304
10. Cohn LB, Silva IT, Oliveira TY, Rosales RA, Parrish EH, Learn GH, et al. HIV-1 integration landscape during latent and active infection. Cell. 2015;160: 420–32. doi:10.1016/j.cell.2015.01.020
11. Delwart EL, Shpaer EG, Louwagie J, McCutchan FE, Grez M, Rübsamen-Waigmann H, et al. Genetic relationships determined by a DNA heteroduplex mobility assay: analysis of HIV-1 env genes. Science. 1993;262: 1257–61.
12. Palmer S, Wiegand AP, Maldarelli F, Bazmi H, Mican JM, Polis M, et al. New real-time reverse transcriptase-initiated PCR assay with single-copy sensitivity for human immunodeficiency virus type 1 RNA in plasma. J Clin Microbiol. 2003;41: 4531–6.
13. Palmer S, Kearney M, Maldarelli F, Halvas EK, Bixby CJ, Bazmi H, et al. Multiple, linked human immunodeficiency virus type 1 drug resistance mutations in treatment-experienced patients are missed by standard genotype analysis. J Clin Microbiol. 2005;43: 406–13. doi:10.1128/JCM.43.1.406-413.2005

14. Bailey JR, Sedaghat AR, Kieffer T, Brennan T, Lee PK, Wind-Rotolo M, et al. Residual human immunodeficiency virus type 1 viremia in some patients on antiretroviral therapy is dominated by a small number of invariant clones rarely found in circulating CD4+ T cells. J Virol. 2006;80: 6441–57. doi:10.1128/JVI.00591-06

15. Salazar-Gonzalez JF, Salazar MG, Keele BF, Learn GH, Giorgi EE, Li H, et al. Genetic identity, biological phenotype, and evolutionary pathways of transmitted/founder viruses in acute and early HIV-1 infection. J Exp Med. 2009;206: 1273–89. doi:10.1084/jem.20090378

16. Herbeck JT, Rolland M, Liu Y, McLaughlin S, McNevin J, Zhao H, et al. Demographic Processes Affect HIV-1 Evolution in Primary Infection before the Onset of Selective Processes. J Virol. 2011;85: 7523–7534. doi:10.1128/JVI.02697-10

17. Evering TH, Mehandru S, Racz P, Tenner-Racz K, Poles MA, Figueroa A, et al. Absence of HIV-1 evolution in the gut-associated lymphoid tissue from patients on combination antiviral therapy initiated during primary infection. PLoS Pathog. 2012;8: e1002506. doi:10.1371/journal.ppat.1002506

18. Wagner TA, McKernan JL, Tobin NH, Tapia KA, Mullins JI, Frenkel LM. An increasing proportion of monotypic HIV-1 DNA sequences during antiretroviral treatment suggests proliferation of HIV-infected cells. J Virol. 2013;87: 1770–8. doi:10.1128/JVI.01985-12

19. Kearney MF, Spindler J, Shao W, Yu S, Anderson EM, O'Shea A, et al. Lack of Detectable HIV-1 Molecular Evolution during Suppressive Antiretroviral Therapy. Siliciano RF, editor. PLoS Pathog. 2014;10: e1004010. doi:10.1371/journal.ppat.1004010

20. Tobin NH, Learn GH, Holte SE, Wang Y, Melvin AJ, McKernan JL, et al. Evidence that low-level viremias during effective highly active antiretroviral therapy result from two processes: expression of archival virus and replication of virus. J Virol. 2005;79: 9625–34. doi:10.1128/JVI.79.15.9625-9634.2005

21. Bull ME, Learn GH, McElhone S, Hitti J, Lockhart D, Holte S, et al. Monotypic human immunodeficiency virus type 1 genotypes across the uterine cervix and in blood suggest proliferation of cells with provirus. J Virol. 2009;83: 6020–8. doi:10.1128/JVI.02664-08

22. Siliciano JD, Siliciano RF. Enhanced culture assay for detection and quantitation of latently infected, resting CD4+ T-cells carrying replication-competent virus in HIV-1-infected individuals. Methods Mol Biol. 2005;304: 3–15. doi:10.1385/1-59259-907-9:003

23. Keele BF, Giorgi EE, Salazar-Gonzalez JF, Decker JM, Pham KT, Salazar MG, et al. Identification and characterization of transmitted and early founder virus envelopes in primary HIV-1 infection. Proc Natl Acad Sci U S A. 2008;105: 7552–7. doi:10.1073/pnas.0802203105

24. Wood N, Bhattacharya T, Keele BF, Giorgi E, Liu M, Gaschen B, et al. HIV evolution in early infection: selection pressures, patterns of insertion and deletion, and the impact of APOBEC. PLoS Pathog. 2009;5: e1000414. doi:10.1371/journal.ppat.1000414

25. Ho Y-C, Shan L, Hosmane NN, Wang J, Laskey SB, Rosenbloom DIS, et al. Replication-competent noninduced proviruses in the latent reservoir increase barrier to HIV-1 cure. Cell. 2013;155: 540–51. doi:10.1016/j.cell.2013.09.020

26. Yu Q, König R, Pillai S, Chiles K, Kearney M, Palmer S, et al. Single-strand specificity of APOBEC3G accounts for minus-strand deamination of the HIV genome. Nat Struct Mol Biol. 2004;11: 435–442. doi:10.1038/nsmb758

27. Suspène R, Rusniok C, Vartanian JP, Wain-Hobson S. Twin gradients in APOBEC3 edited HIV-1 DNA reflect the dynamics of lentiviral replication. Nucleic Acids Res. 2006;34: 4677–4684. doi:10.1093/nar/gkl555

28. Jabara CB, Jones CD, Roach J, Anderson JA, Swanstrom R. Accurate sampling and deep sequencing of the HIV-1 protease gene using a Primer ID. Proc Natl Acad Sci. 2011;108: 20166–20171. doi:10.1073/pnas.1110064108

29. Bruner K. *et al*. Rapid accumulation of defective proviruses complicates HIV-1 reservoir measurements. In press with Nature Medicine in June 2016.

30. Laskey SB, Pohlmeyer CW, Bruner K, Siliciano R. Evaluating clonal expansion of HIV-infected cells: optimization of PCR strategies to predict clonality. In press with *PLoS Pathog* in June 2016.

31. van Lunzen J, Maggiolo F, Arribas JR, Rakhmanova A, Yeni P, Young B, et al. Once daily dolutegravir (S/GSK1349572) in combination therapy in antiretroviral-naive adults with HIV: planned interim 48 week results from SPRING-1, a dose-ranging, randomised, phase 2b trial. Lancet Infect Dis. 2012;12: 111–8. doi:10.1016/S1473-3099(11)70290-0

32. Walmsley SL, Antela A, Clumeck N, Duiculescu D, Eberhard A, Gutiérrez F, et al. Dolutegravir plus abacavir-lamivudine for the treatment of HIV-1 infection. N Engl J Med. 2013;369: 1807–18. doi:10.1056/NEJMoa1215541

33. Raffi F, Jaeger H, Quiros-Roldan E, Albrecht H, Belonosova E, Gatell JM, et al. Once-daily dolutegravir versus twice-daily raltegravir in antiretroviral-naive adults with HIV-1 infection (SPRING-2 study): 96 week results from a randomised, double-blind, non-inferiority trial. Lancet Infect Dis. 2013;13: 927–35. doi:10.1016/S1473-3099(13)70257-3

34. Clotet B, Feinberg J, van Lunzen J, Khuong-Josses M-A, Antinori A, Dumitru I, et al. Once-daily dolutegravir versus darunavir plus ritonavir in antiretroviral-naive adults with HIV-1 infection (FLAMINGO): 48 week results from the randomised open-label phase 3b study. Lancet (London, England). 2014;383: 2222–31. doi:10.1016/S0140-6736(14)60084-2

35. Bollen P, Reiss P, Schapiro J, Burger D. Clinical pharmacokinetics and pharmacodynamics of dolutegravir used as a single tablet regimen for the treatment of HIV-1 infection. Expert Opin Drug Saf. 2015;14: 1457–72. doi:10.1517/14740338.2015.1059818

36. Despiégel N, Anger D, Martin M, Monga N, Cui Q, Rocchi A, et al. Cost-Effectiveness of Dolutegravir in HIV-1 Treatment-Naive and Treatment-Experienced Patients in Canada. Infect Dis Ther. 2015;4: 337–53. doi:10.1007/s40121-015-0071-0

37. Malet I, Thierry E, Wirden M, Lebourgeois S, Subra F, Katlama C, et al. Combination of two pathways involved in raltegravir resistance confers dolutegravir resistance. J Antimicrob Chemother. 2015;70: 2870–80. doi:10.1093/jac/dkv197

38. Liang J, Mesplède T, Oliveira M, Anstett K, Wainberg MA. The Combination of the R263K and T66I Resistance Substitutions in HIV-1 Integrase Is Incompatible with High-Level Viral Replication and

the Development of High-Level Drug Resistance. J Virol. 2015;89: 11269–74. doi:10.1128/JVI.01881-15

39. Shen L, Peterson S, Sedaghat AR, McMahon M a, Callender M, Zhang H, et al. Dose-response curve slope sets class-specific limits on inhibitory potential of anti-HIV drugs. Nat Med. 2008;14: 762–6. doi:10.1038/nm1777

40. Jilek BL, Zarr M, Sampah ME, Rabi SA, Bullen CK, Lai J, et al. A quantitative basis for antiretroviral therapy for HIV-1 infection. Nat Med. Nature Publishing Group; 2012;18: 446–51. doi:10.1038/nm.2649

41. Desimmie BA, Schrijvers R, Demeulemeester J, Borrenberghs D, Weydert C, Thys W, et al. LEDGINs inhibit late stage HIV-1 replication by modulating integrase multimerization in the virions. Retrovirology. 2013;10: 57. doi:10.1186/1742-4690-10-57

42. Le Rouzic E, Bonnard D, Chasset S, Bruneau J-M, Chevreuil F, Le Strat F, et al. Dual inhibition of HIV-1 replication by integrase-LEDGF allosteric inhibitors is predominant at the post-integration stage. Retrovirology. 2013;10: 144. doi:10.1186/1742-4690-10-144

43. Balakrishnan M, Yant SR, Tsai L, O'Sullivan C, Bam RA, Tsai A, et al. Non-catalytic site HIV-1 integrase inhibitors disrupt core maturation and induce a reverse transcription block in target cells. PLoS One. 2013;8: e74163. doi:10.1371/journal.pone.0074163

44. Jurado K, Wang H, Slaughter A, Feng L, Kessl JJ, Koh Y, et al. Allosteric integrase inhibitor potency is determined through the inhibition of HIV-1 particle maturation. Proc Natl Acad Sci U S A. 2013;110: 8690–5. doi:10.1073/pnas.1300703110

45. Gupta K, Brady T, Dyer BM, Malani N, Hwang Y, Male F, et al. Allosteric inhibition of human immunodeficiency virus integrase: late block during viral replication and abnormal multimerization involving specific protein domains. J Biol Chem. 2014;289: 20477–88. doi:10.1074/jbc.M114.551119

46. Panel on Antiretroviral Guidelines for Adults and Adolescents. Guidelines for the use of antiretroviral agents in HIV-1-infected adults and adolescents. Department of Health and Human Services. Available at http://aidsinfo.nih.gov/contentfiles/lvguidelines/AdultandAdolescentGL.pdf. Section accessed April 11, 2016.

47. Loewe S, Muischnek H. 1926. Effect of combinations: mathematical basis of problem. Arch Exp Pathol Pharmakol 114:313-326.

48. Bliss C. The toxicity of poisons applied jointly. Ann Appl Biol. 1939; 585–615.

49. Sued OG, Figueroa MI, Rolon MJ, Patterson P, Brown D, Gun AM, Aboud M, Smith KY, Cahn P. Comparable Viral Decay in Dual and Triple Dolutegravir-Based Antiretroviral Therapy. CROI Conference 2016 Abstract 947.

50. Sampah MES, Shen L, Jilek BL, Siliciano RF. Dose-response curve slope is a missing dimension in the analysis of HIV-1 drug resistance. Proc Natl Acad Sci U S A. 2011;108: 7613–8. doi:10.1073/pnas.1018360108

51. Shadrina OA, Zatsepin TS, Agapkina YY, Isaguliants MG, Gottikh MB. Influence of Drug Resistance Mutations on the Activity of HIV-1 Subtypes A and B Integrases: a Comparative Study. Acta Naturae. 7: 78–86.

52. Rabi SA, Laird GM, Durand CM, Laskey S, Shan L, Bailey JR, et al. Multi-step inhibition explains HIV-1 protease inhibitor pharmacodynamics and resistance. J Clin Invest. 2013;123: 3848–60. doi:10.1172/JCI67399

53. Laskey SB, Siliciano RF. A mechanistic theory to explain the efficacy of antiretroviral therapy. Nat Rev Microbiol. Nature Publishing Group, a division of Macmillan Publishers Limited. All Rights Reserved.; 2014;12: 772–80. doi:10.1038/nrmicro3351

54. Zhang H, Zhou Y, Alcock C, Kiefer T, Monie D, Siliciano J, et al. Novel Single-Cell-Level Phenotypic Assay for Residual Drug Susceptibility and Reduced Replication Capacity of Drug-Resistant Human Immunodeficiency Virus Type 1. J Virol. 2004;78: 1718–1729. doi:10.1128/JVI.78.4.1718-1729.2004

55. ViiV Healthcare Company. 2013. TIVICAY (Dolutegravir) prescribing information.

CURRICULUM VITAE

The Johns Hopkins University School of Medicine

Sarah Laskey June 2016

Educational History:

Ph.D. expected	2016	Biomedical Engineering Johns Hopkins School of Medicine Mentor: Robert Siliciano
B.S.	2011	Biological Engineering Massachusetts Institute of Technology

Professional Experience:

Research rotation	2012	Lab of Stuart Ray Johns Hopkins School of Medicine
Undergraduate research	2009-2011	Lab of Phillip Sharp Massachusetts Institute of Technology
Undergraduate research	2010	Lab of Mayuree Fuangthong Chulabhorn Research Institute
Software engineer	2006-2008	Digital Sandbox

Scholarships:

Young Investigator Scholarship	2016	Conference on Retroviruses and Opportunistic Infections
William and Mary Drescher Scholarship	2012	Johns Hopkins School of Medicine

Publications:

- **Laskey SB**, Hill AL, Siliciano RF & Rosenbloom DIS. Re-evaluating evolution in the HIV reservoir. *Nature, BCA manuscript submitted.*
- **Laskey SB** & Siliciano RF. Antiretroviral efficacy of dolutegravir alone and in combination against wild-type and drug-resistant HIV-1. *Manuscript in preparation.*
- Hosmane NN, Kwon KJ, **Laskey SB**, Capoferri AA, Ho YC, Siliciano JD & Siliciano RF. Multiple rounds of maximum T cell activation induce additional replication-competent HIV-1 from resting memory $CD4^+$ T cells. *Manuscript in preparation*.
- Pohlmeyer CW, **Laskey S**, Xu D, Longwich AZ, Lichmira W, Siliciano RF & Blankson JN. Modulation of HIV-specific CTL populations using cross-reactive microbial peptides. *Manuscript in preparation.*
- **Laskey SB**, Pohlmeyer CW, Bruner K & Siliciano RF. Optimization of PCR amplicons to predict clonality of full-length HIV-1 sequences. *Under revision with PLoS Path.*
- Bruner K, Pollack R, Murray A, Soliman M, **Laskey SB**, Capoferri A, Lai J, Strain M, Lada S, Hoh R, Ho YC, Richman DD, Deeks S, Siliciano JD & Siliciano RF. Unbiased screen reveals rapid accumulation of defective proviruses thus complicating HIV-1 reservoir measurements. *Under revision with Nat Med.*

- Gray WT, Frey KM, **Laskey SB**, Mislak AC, Spasov KA, Lee WG, Bollini M, Siliciano RF, Jorgensen WL & Anderson KS. (2015). Potent inhibitors active against HIV reverse transcriptase with K101P, a mutation conferring rilpivirine resistance. *ACS Med Chem Lett.*
- **Laskey SB** & Siliciano RF. (2014). A mechanistic theory to explain the efficacy of antiretroviral therapy. *Nat Rev Microbiol.*
- Rabi SA, Laird GM, Durand CM, **Laskey S**, Shan L, Bailey JR, Chioma S, Moore RD & Siliciano RF. (2013). Multi-step inhibition explains HIV-1 protease inhibitor pharmacodynamics and resistance. *J Clin Invest.*
- Ho YC, Shan L, Hosmane NN, Wang J, **Laskey SB**, Rosenbloom DI, Lai J, Blankson JN, Siliciano JD & Siliciano RF. (2013). Replication-competent noninduced proviruses in the latent reservoir increase barrier to HIV-1 cure. *Cell.*
- Bailey JR, **Laskey S**, Wasilewski LN, Munshaw S, Fanning LJ, Kenny-Walsh E, Ray SC. (2012). *J Virol.*

Posters:

- **Laskey SB** & Siliciano RF. The high *in vivo* efficacy of raltegravir cannot be explained by drug activity at posttranslational steps of the HIV-1 life cycle. CARE Conference 2014.
- **Laskey SB**, Pohlmeyer CW, Elliott O, Bruner KM & Siliciano RF. Optimization of PCR Amplicons to Predict Clonality of Full-Length HIV-1 Sequences. CROI 2016.
- **Laskey SB** & Siliciano RF. A Quantitative Model of ART Efficacy Explains the Clinical Success of Dolutegravir. CROI 2016.
- Bruner KM, Pollack R, Murray A, Soliman M, **Laskey SB**, Strain MF, Richman DD, Deeks SG, Siliciano J & Siliciano R. Rapid Accumulation of Defective Proviruses Complicates HIV-1 Reservoir Measurements. CROI 2016.